Origin of silica in rice plants and contribution of diatom Earth fertilization : insights from isotopic Si mass balance in a paddy field

Jean Riotte, Kollalu Sandhya, Nagabovanalli B. Prakash, Stephane Audry, Thomas Zambardi, Jerome Chmeleff, Sriramulu Buvaneshwari, Jean-Dominique Meunier

Origin of silica in rice plants and contribution of diatom earth fertilization: insights from isotopic Si mass balance in a paddy field

Jean Riotte[1,2*], Kollalu Sandhya[3], Nagabovanalli B. Prakash[3], Stéphane Audry[1], Thomas Zambardi[1], Jérôme Chmeleff[1], Sriramulu Buvaneshwari[4] Jean-Dominique Meunier[5]

(*) Corresponding author: jean.riotte@ird.fr

1- Géosciences Environnement Toulouse (Université Paul-Sabatier, IRD, CNRS), 14 avenue E. Belin, 31400 Toulouse, France

2- Indo-French Cell for Water Sciences, IRD-Indian Institute of Science, Bangalore 560012 India

3- University of Agricultural Sciences, GKVK, Bangalore, India

4- (1) Indian Institute of Science, Department of Civil Engineering, 560012 Bengaluru, India

5- Aix Marseille Univ, CNRS, IRD, Coll France, CEREGE, 13545 Aix-en-Provence cedex 04, France

Abstract

Background and aims

The benefits of Si for crops is well evidenced but the biogeochemical cycle of Si in agriculture remains poorly documented. This study aims at identifying and quantifying the Si sources (primary and secondary soil minerals, amorphous silica, irrigation, Si-fertilizer) to rice plants.

Method

Field experiments were carried out with and without application of diatomaceous earth (DE) under rice and bare conditions to determine the water and dissolved mass balance in paddy fields (Karnataka, Southern India). The fate of the Si brought by irrigation (DSi) (uptake by rice, uptake by diatoms, adsorption) was assessed through a solute mass balance combined with silicon isotopic signatures.

Results

Above the ground-surface, about one third of the DSi flux brought by borewell irrigation (545 mmol $Si.m^{-2}$) to bare plots and half of DSi in rice plots were removed from solution within minutes or hours following irrigation. Such rate is consistent with the rate of DSi adsorption onto Fe-oxyhydroxides but not with diatom blooms. In rice and rice+DE experiments, the

Figure 1

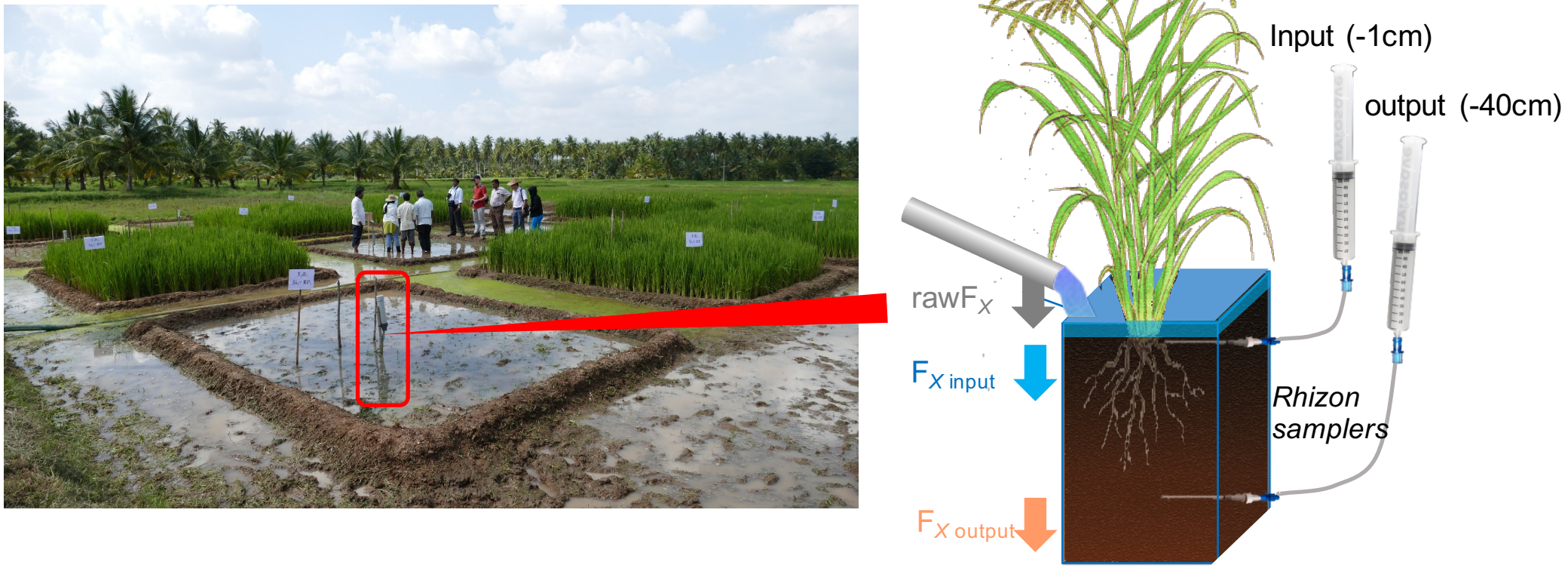
Input (-1cm)
output (-40cm)
rawF$_X$
F$_X$ input
F$_X$ output
Rhizon samplers

Figure 2

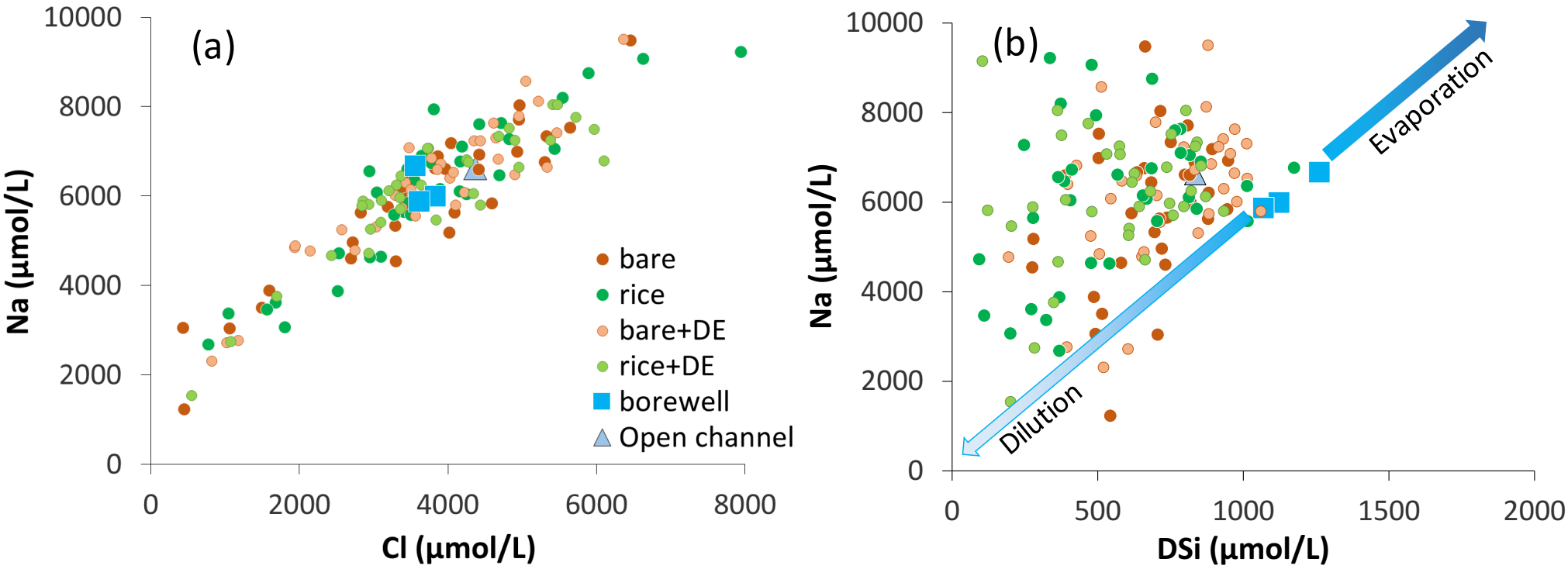
(a)
Na (µmol/L)
Cl (µmol/L)
0
2000
4000
6000
8000
10000
bare
rice
bare+DE
rice+DE
borewell
Open channel
(b)
Na (µmol/L)
DSi (µmol/L)
0
500
1000
1500
2000
Evaporation
Dilution

Figure 2

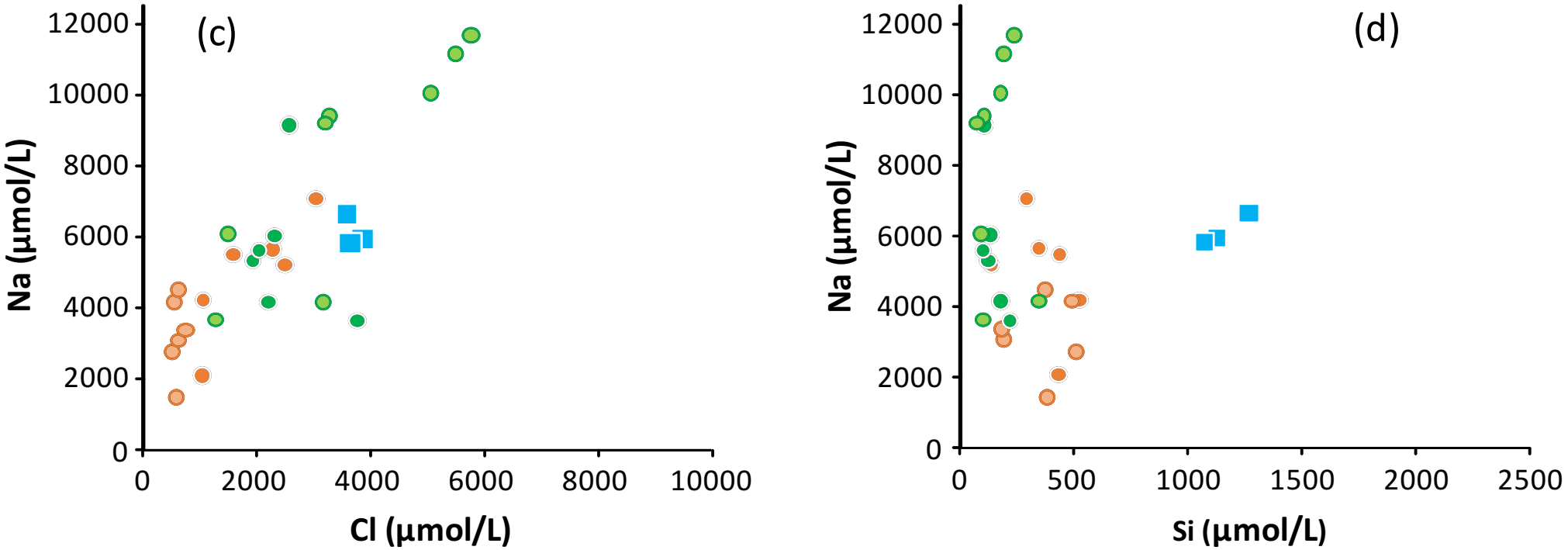
(c)
12000
10000
8000
6000
4000
2000
0
Na (µmol/L)
0
2000
4000
6000
8000
10000
Cl (µmol/L)
(d)
12000
10000
8000
6000
4000
2000
0
Na (µmol/L)
0
500
1000
1500
2000
2500
Si (µmol/L)

Figure 3

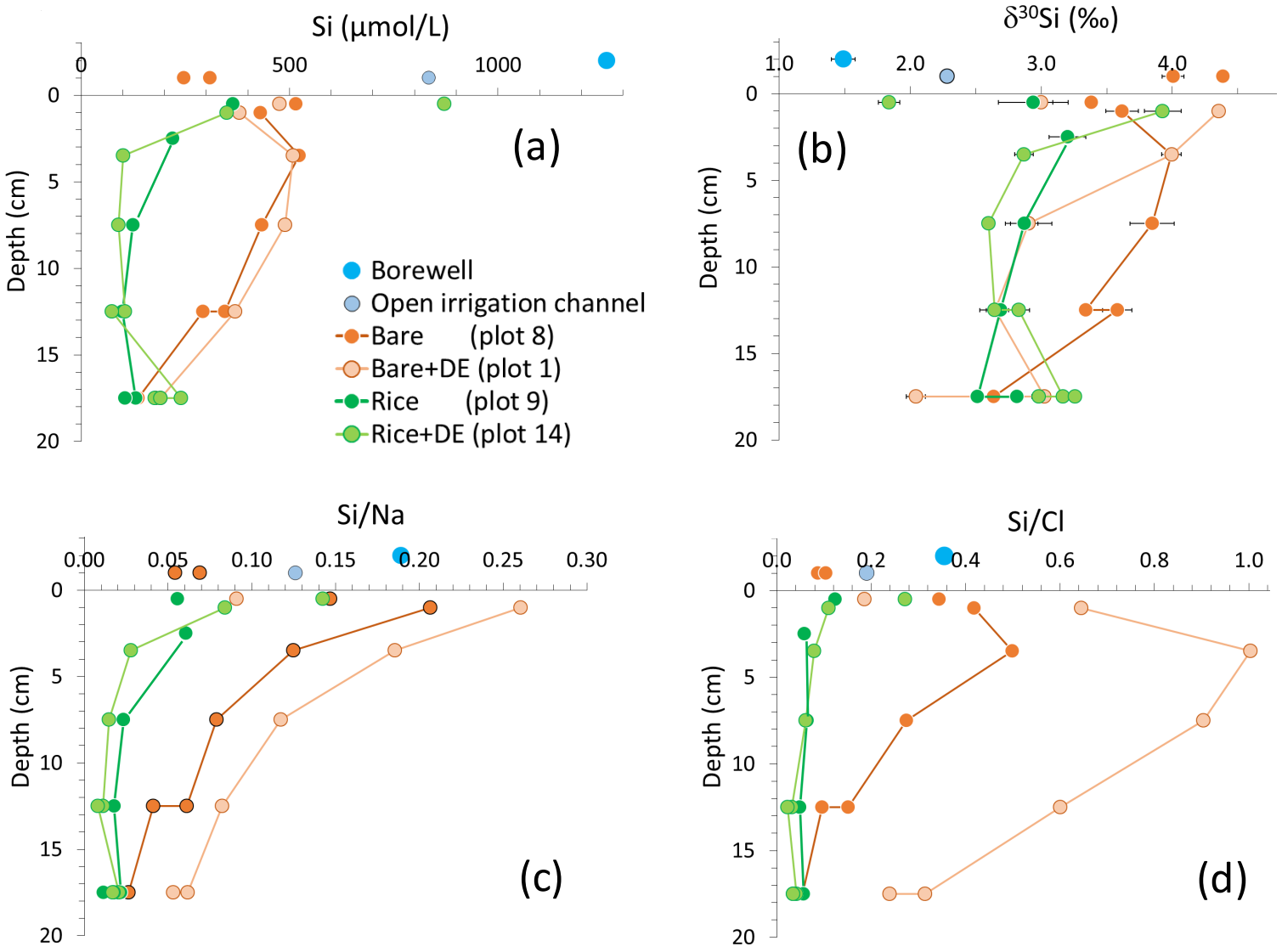
Si (µmol/L)
0
500
1000
Depth (cm)
0
5
10
15
20
(a)
Borewell
Open irrigation channel
Bare (plot 8)
Bare+DE (plot 1)
Rice (plot 9)
Rice+DE (plot 14)
δ30Si (‰)
1.0
2.0
3.0
4.0
(b)
Si/Na
0.00
0.05
0.10
0.15
0.20
0.25
0.30
(c)
Si/Cl
0.0
0.2
0.4
0.6
0.8
1.0
(d)

Figure 4

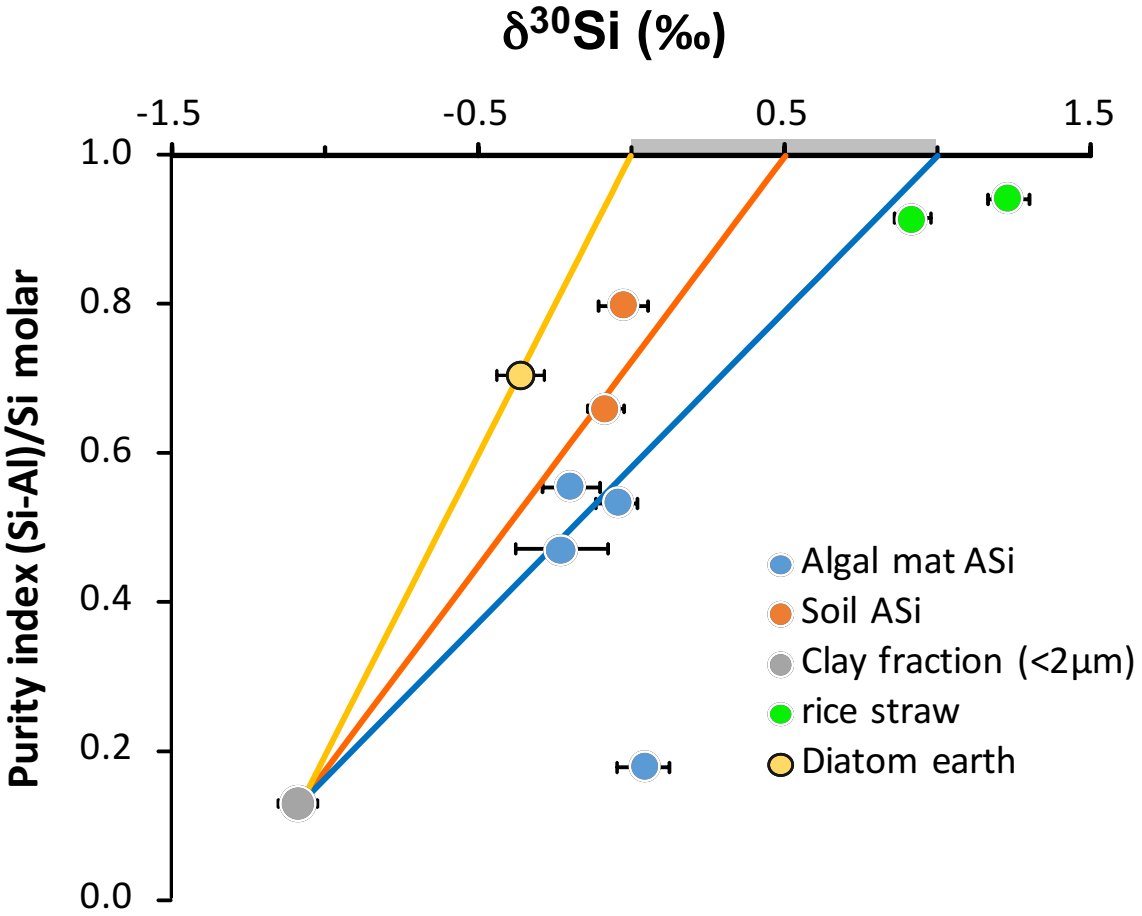
δ30Si (‰)
-1.5
-0.5
0.5
1.5
1.0
0.8
0.6
0.4
0.2
0.0
Purity index (Si-Al)/Si molar
Algal mat ASi
Soil ASi
Clay fraction (<2µm)
rice straw
Diatom earth

Figure 5

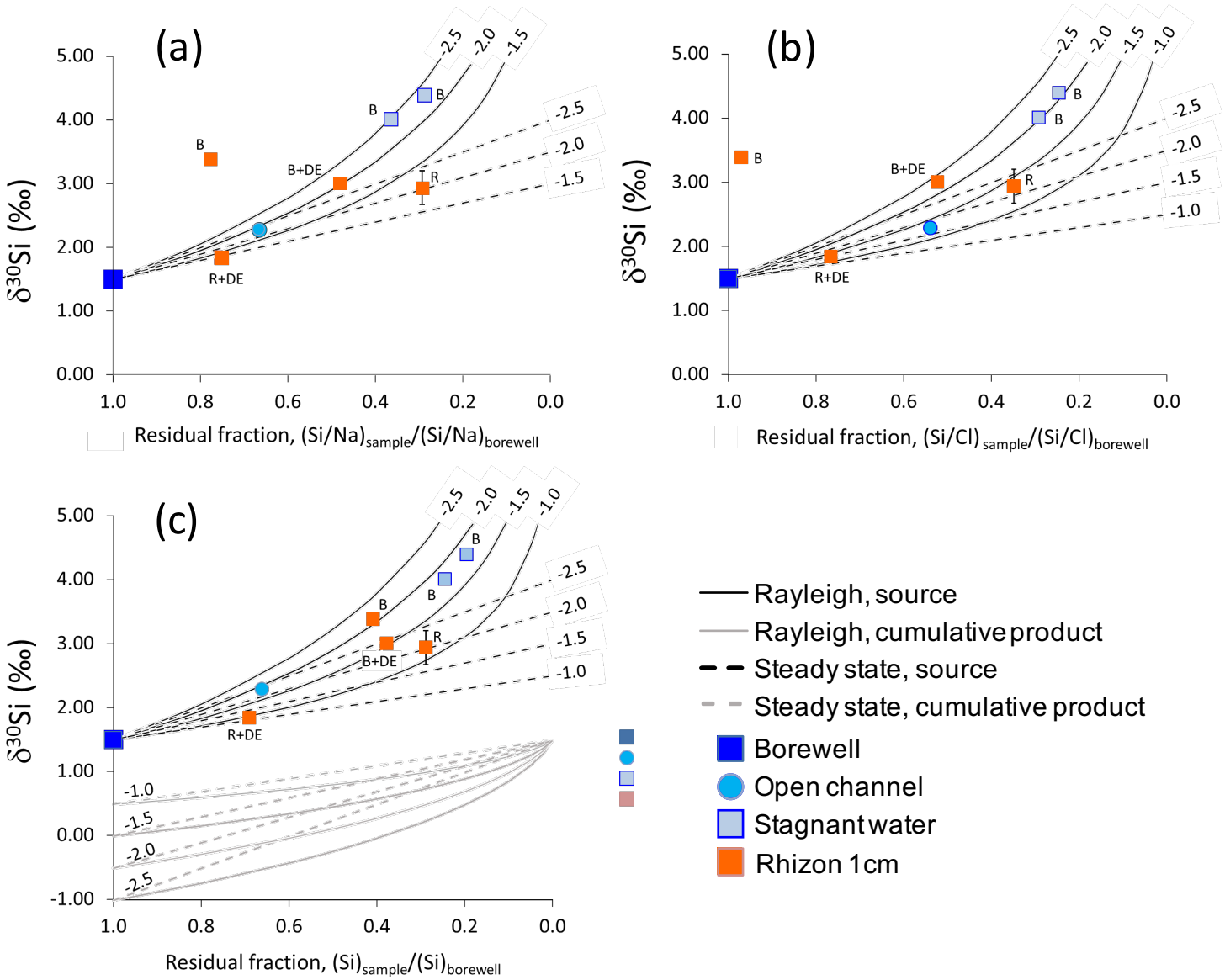
(a)
(b)
(c)
δ30Si (‰)
Residual fraction, (Si/Na)sample/(Si/Na)borewell
Residual fraction, (Si/Cl)sample/(Si/Cl)borewell
Residual fraction, (Si)sample/(Si)borewell
B
B+DE
R+DE
R
-2.5
-2.0
-1.5
-1.0
Rayleigh, source
Rayleigh, cumulative product
Steady state, source
Steady state, cumulative product
Borewell
Open channel
Stagnant water
Rhizon 1cm

Figure 6

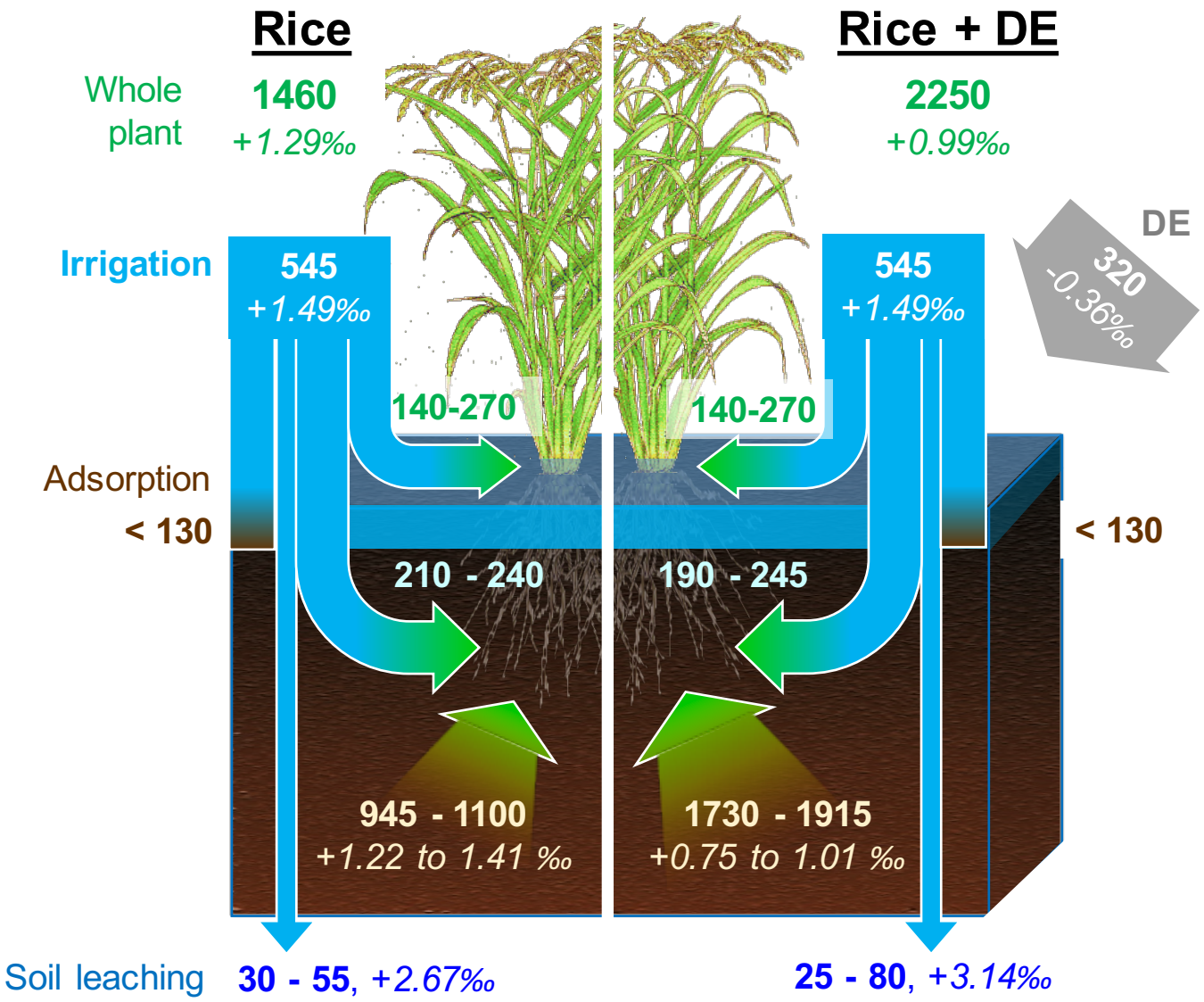
Rice
Rice + DE
Whole plant
1460
+1.29‰
2250
+0.99‰
DE
320
-0.36‰
Irrigation
545
+1.49‰
545
+1.49‰
140-270
140-270
Adsorption
< 130
< 130
210 - 240
190 - 245
945 - 1100
+1.22 to 1.41 ‰
1730 - 1915
+0.75 to 1.01 ‰
Soil leaching
30 - 55, +2.67‰
25 - 80, +3.14‰

Figure 6 = schema synthetique avec flux possibles

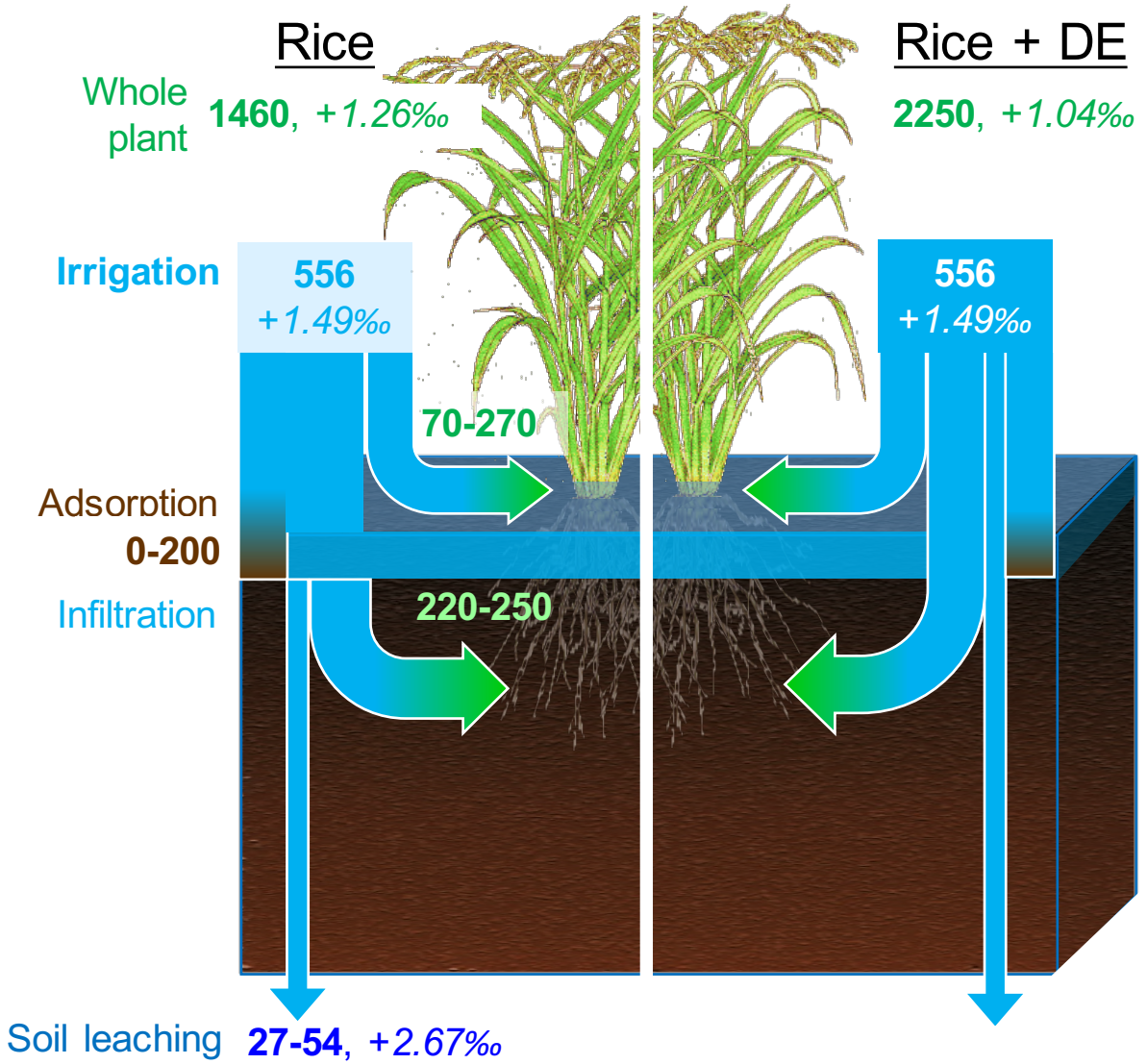

Figure 6 = schema synthetique avec flux possibles

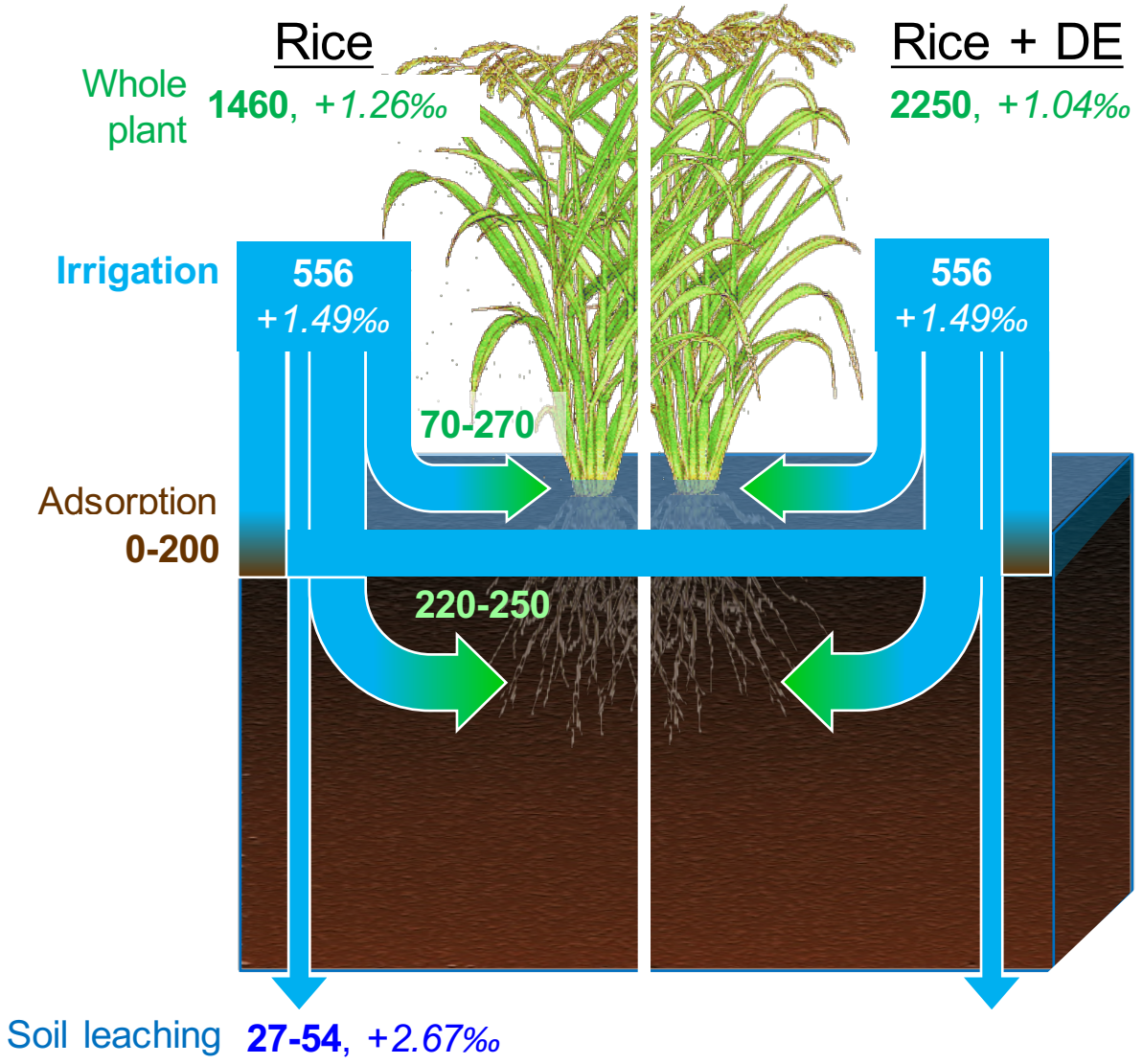

Figure 6 = schema synthetique avec flux possibles

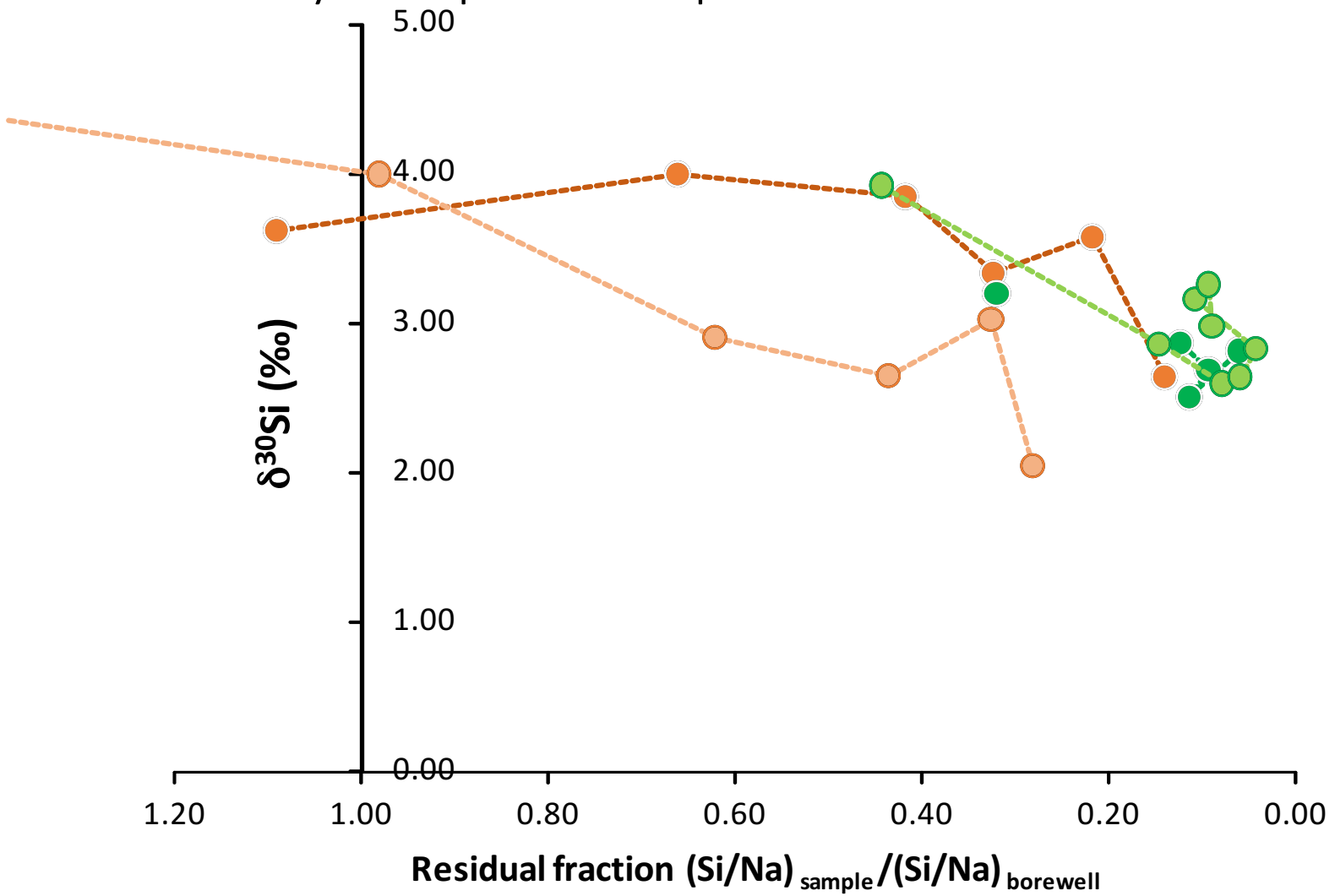

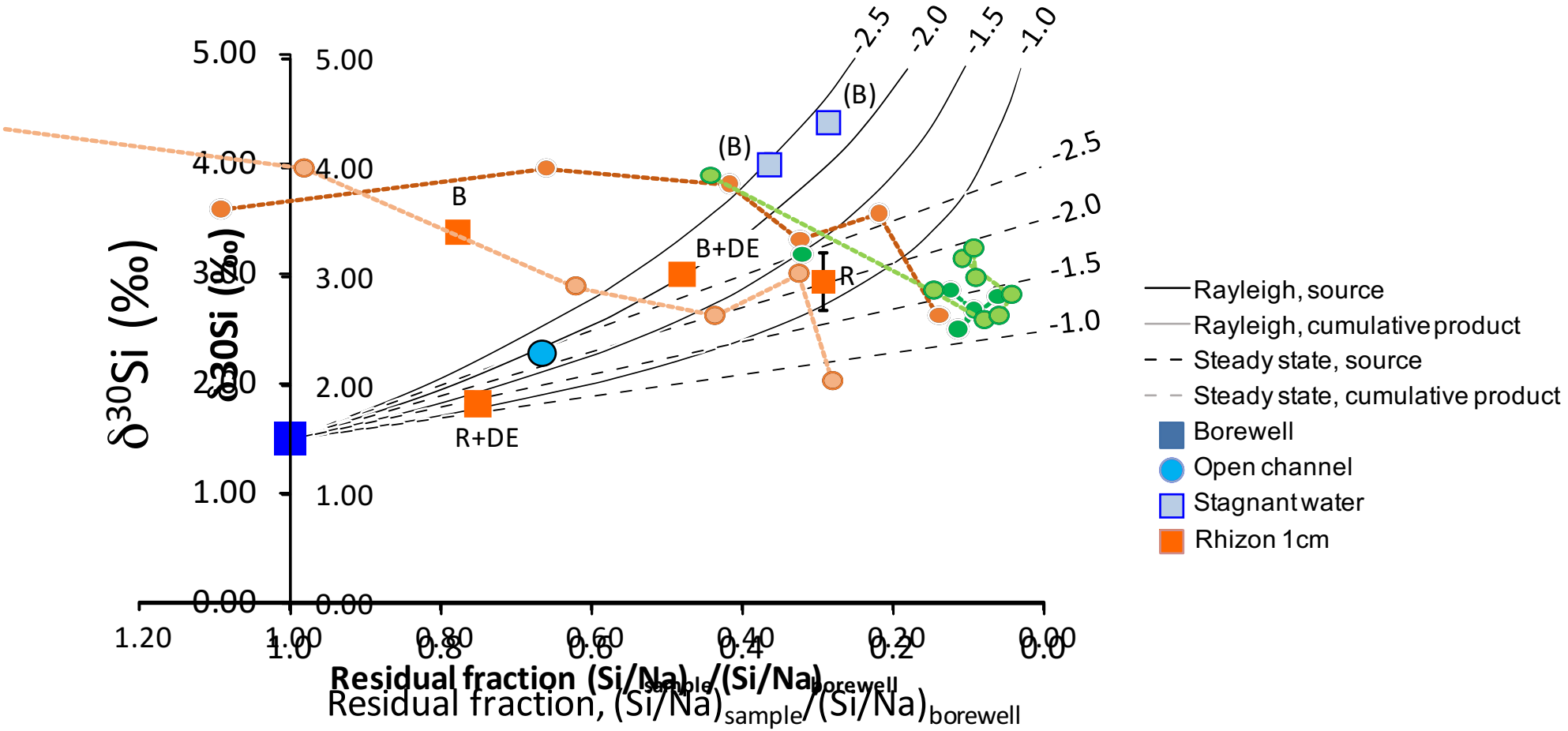
5.00
4.00
3.00
2.00
1.00
0.00
δ30Si (‰)
1.20
1.00
0.80
0.60
0.40
0.20
0.00
Residual fraction, (Si/Na)sample/(Si/Na)borewell
-2.5
-2.0
-1.5
-1.0
(B)
B
B+DE
R
R+DE
Rayleigh, source
Rayleigh, cumulative product
Steady state, source
Steady state, cumulative product
Borewell
Open channel
Stagnant water
Rhizon 1cm

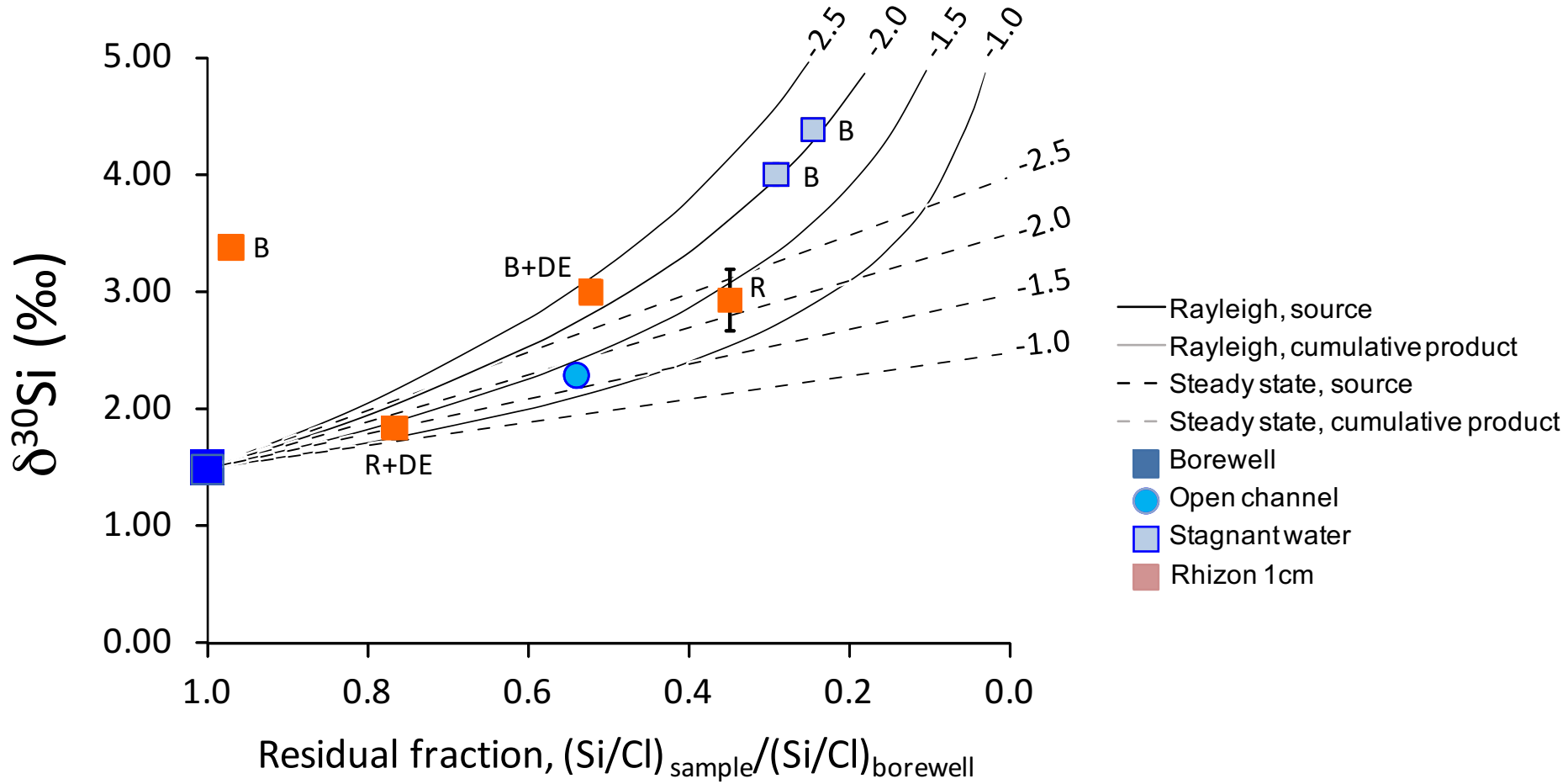
5.00
4.00
3.00
2.00
1.00
0.00
1.0
0.8
0.6
0.4
0.2
0.0
δ30Si (‰)
Residual fraction, (Si/Cl) sample/(Si/Cl)borewell
-2.5
-2.0
-1.5
-1.0
B
B
B
B+DE
R
R+DE
-2.5
-2.0
-1.5
-1.0
Rayleigh, source
Rayleigh, cumulative product
Steady state, source
Steady state, cumulative product
Borewell
Open channel
Stagnant water
Rhizon 1cm

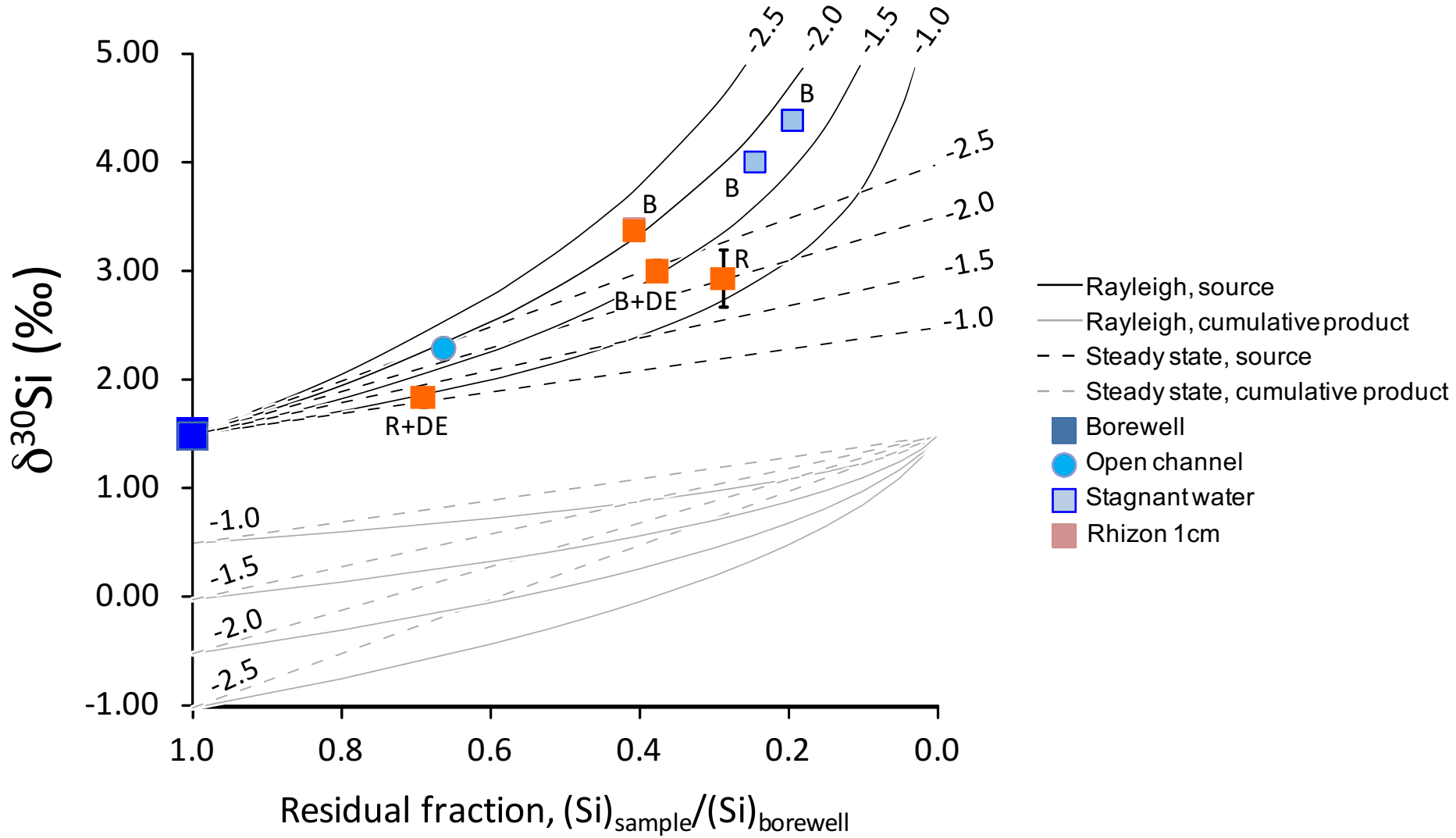
5.00
4.00
3.00
2.00
1.00
0.00
-1.00
1.0
0.8
0.6
0.4
0.2
0.0
δ30Si (‰)
Residual fraction, (Si)sample/(Si)borewell
-2.5
-2.0
-1.5
-1.0
B
B
B
B+DE
R
R+DE
-2.5
-2.0
-1.5
-1.0
-1.0
-1.5
-2.0
-2.5
Rayleigh, source
Rayleigh, cumulative product
Steady state, source
Steady state, cumulative product
Borewell
Open channel
Stagnant water
Rhizon 1cm

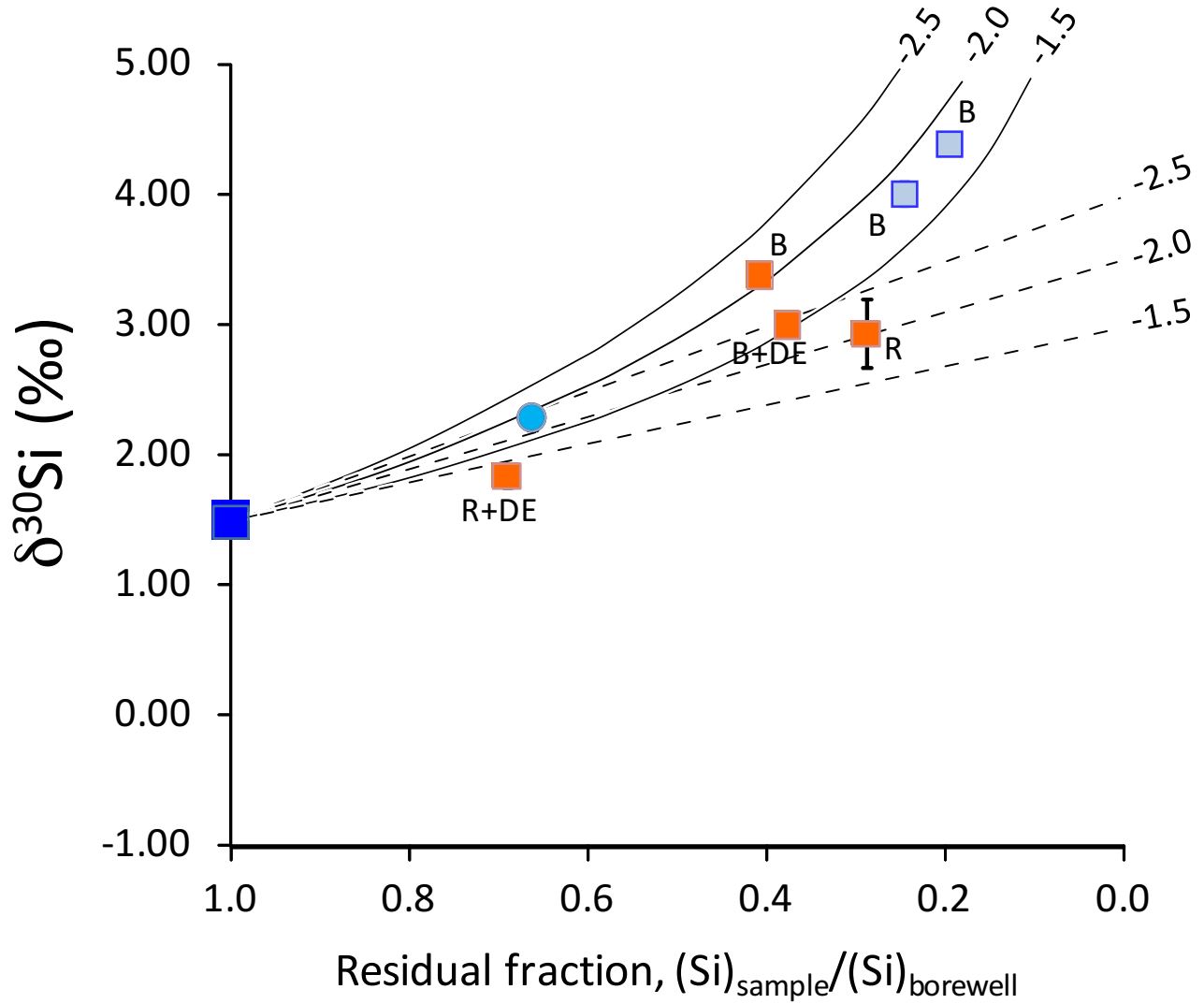
5.00
4.00
3.00
2.00
1.00
0.00
-1.00
1.0
0.8
0.6
0.4
0.2
0.0
δ30Si (‰)
Residual fraction, (Si)sample/(Si)borewell
-2.5
-2.0
-1.5
B
B
B
B+DE
R
R+DE
-2.5
-2.0
-1.5

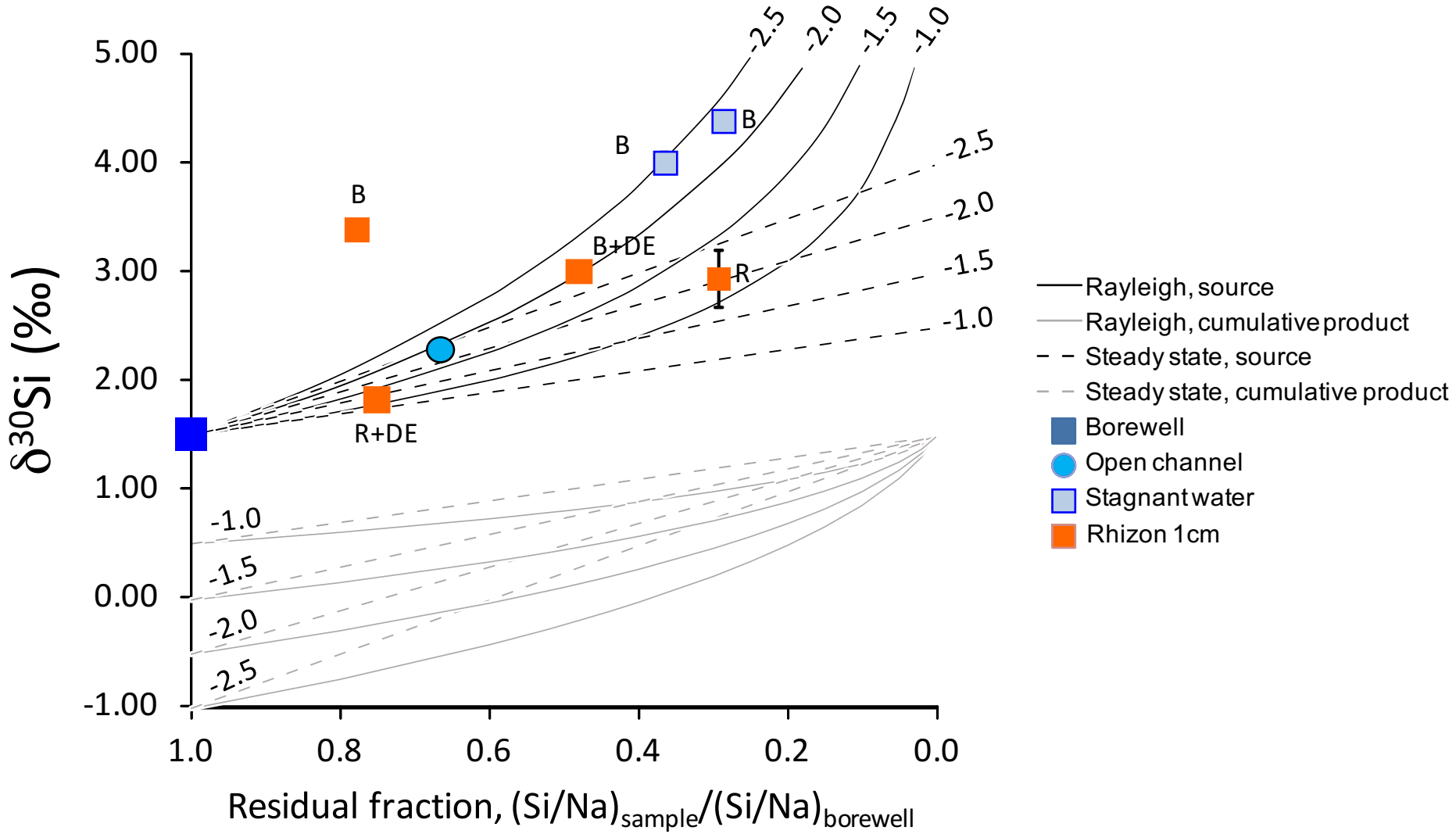
5.00
4.00
3.00
2.00
1.00
0.00
-1.00
δ30Si (‰)
1.0
0.8
0.6
0.4
0.2
0.0
Residual fraction, (Si/Na)sample/(Si/Na)borewell
-2.5
-2.0
-1.5
-1.0
B
B
B
B+DE
R
R+DE
-1.0
-1.5
-2.0
-2.5
-2.5
-2.0
-1.5
-1.0
Rayleigh, source
Rayleigh, cumulative product
Steady state, source
Steady state, cumulative product
Borewell
Open channel
Stagnant water
Rhizon 1cm

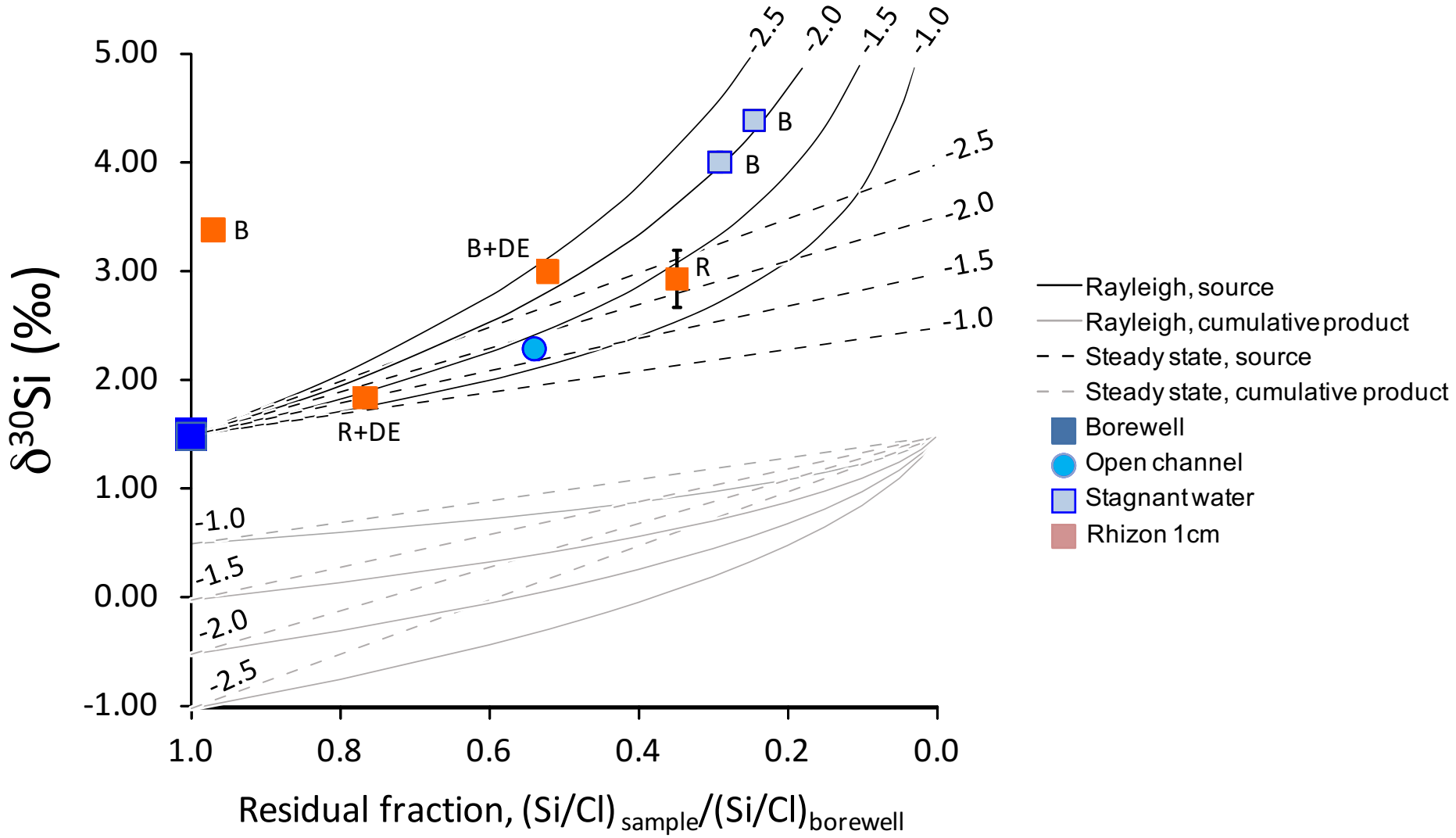
5.00
4.00
3.00
2.00
1.00
0.00
-1.00
δ30Si (‰)
1.0
0.8
0.6
0.4
0.2
0.0
Residual fraction, (Si/Cl) sample/(Si/Cl)borewell
B
B
B
B+DE
R
R+DE
-2.5
-2.0
-1.5
-1.0
-2.5
-2.0
-1.5
-1.0
-1.0
-1.5
-2.0
-2.5
Rayleigh, source
Rayleigh, cumulative product
Steady state, source
Steady state, cumulative product
Borewell
Open channel
Stagnant water
Rhizon 1cm

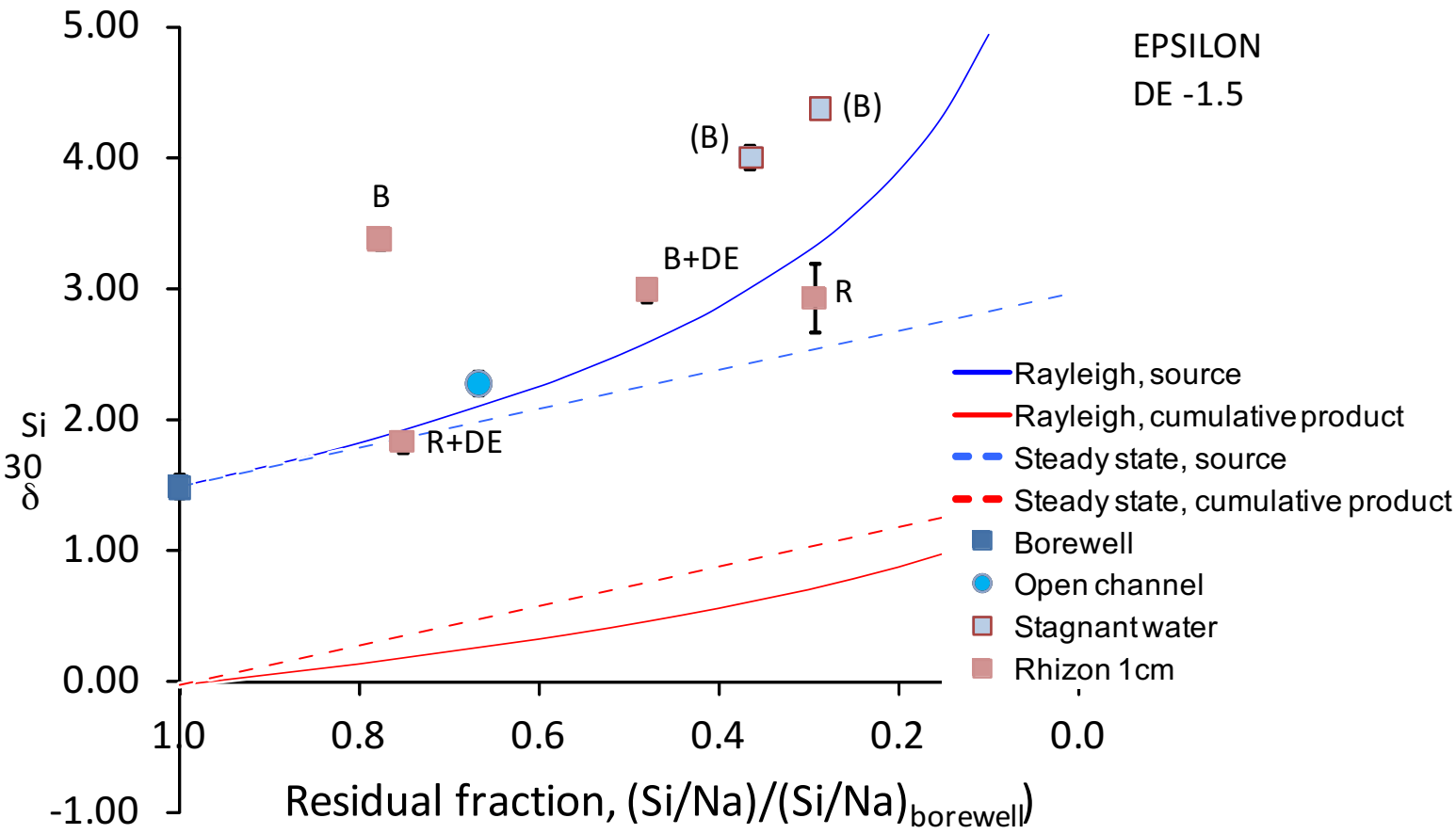
5.00
4.00
3.00
2.00
1.00
0.00
-1.00
Si 30 δ
1.0
0.8
0.6
0.4
0.2
0.0
Residual fraction, (Si/Na)/(Si/Na)borewell)
B
(B)
(B)
B+DE
R
R+DE
EPSILON
DE -1.5
Rayleigh, source
Rayleigh, cumulative product
Steady state, source
Steady state, cumulative product
Borewell
Open channel
Stagnant water
Rhizon 1cm

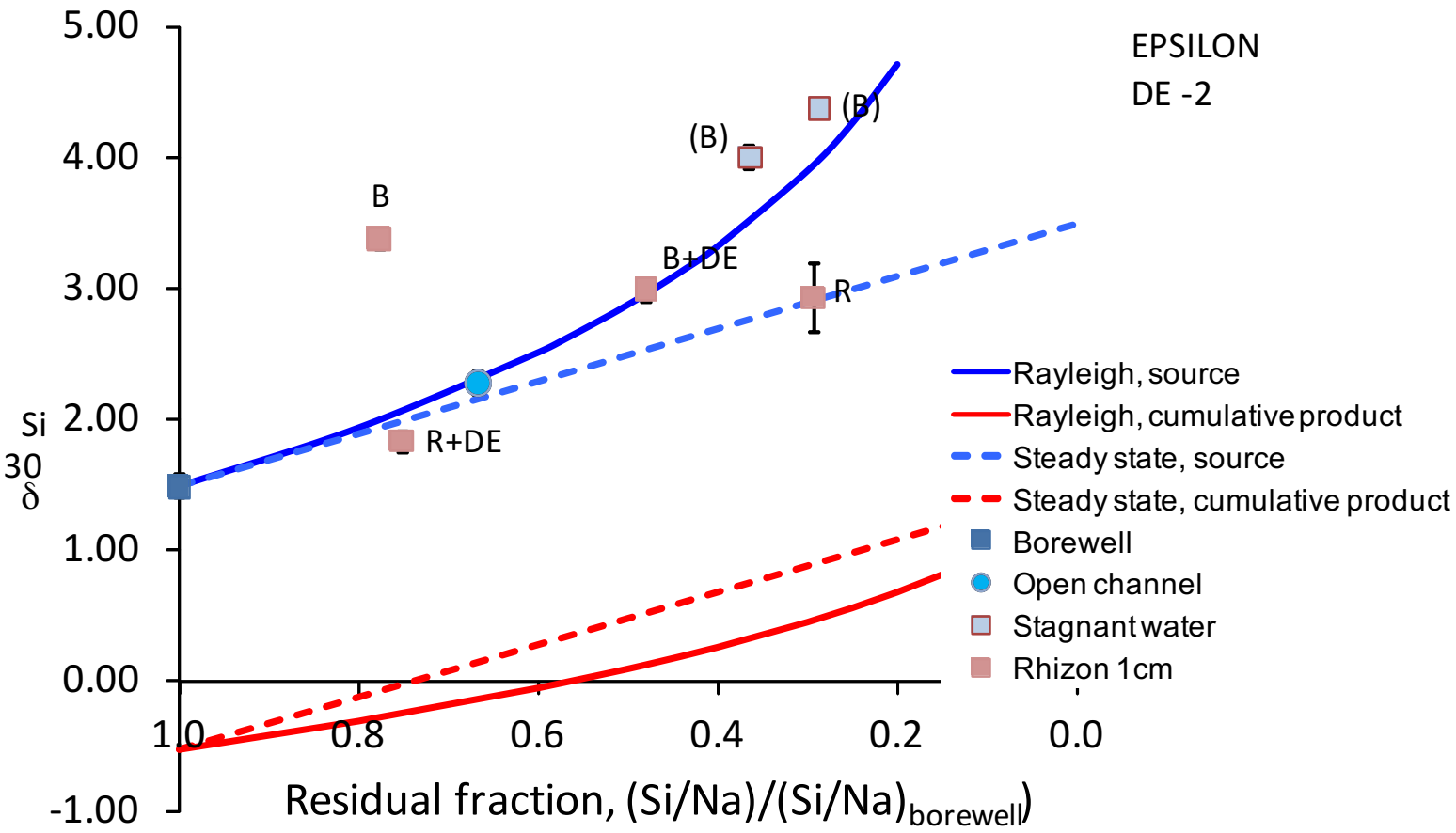
EPSILON
DE -2
5.00
4.00
3.00
2.00
1.00
0.00
-1.00
Si 30 δ
1.0
0.8
0.6
0.4
0.2
0.0
Residual fraction, (Si/Na)/(Si/Na)borewell
B
(B)
(B)
B+DE
R
R+DE
Rayleigh, source
Rayleigh, cumulative product
Steady state, source
Steady state, cumulative product
Borewell
Open channel
Stagnant water
Rhizon 1cm

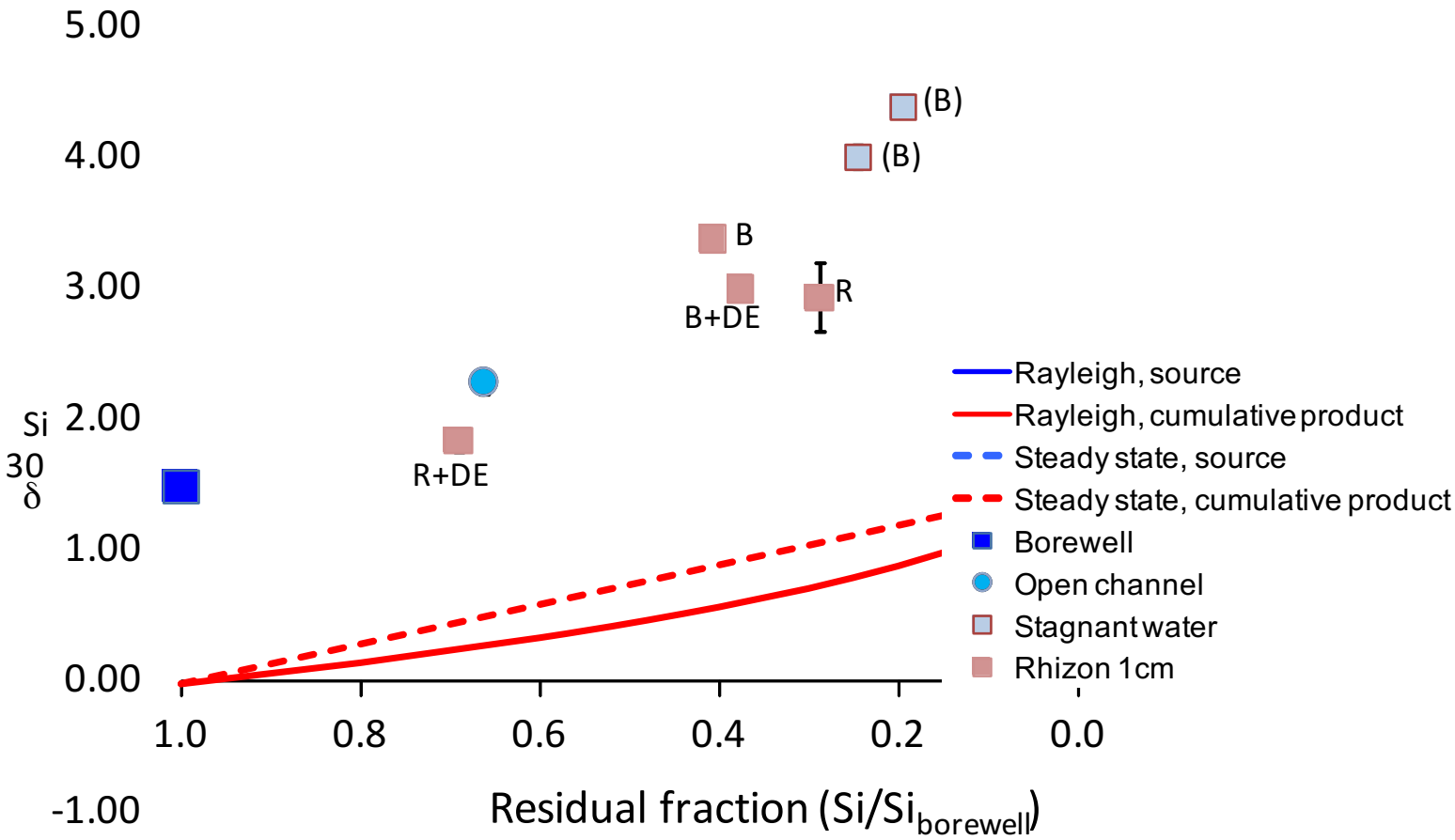
5.00
4.00
3.00
2.00
1.00
0.00
-1.00
Si 30 δ
(B)
(B)
B
B+DE
R
R+DE
1.0
0.8
0.6
0.4
0.2
0.0
Residual fraction (Si/Si borewell)
Rayleigh, source
Rayleigh, cumulative product
Steady state, source
Steady state, cumulative product
Borewell
Open channel
Stagnant water
Rhizon 1cm

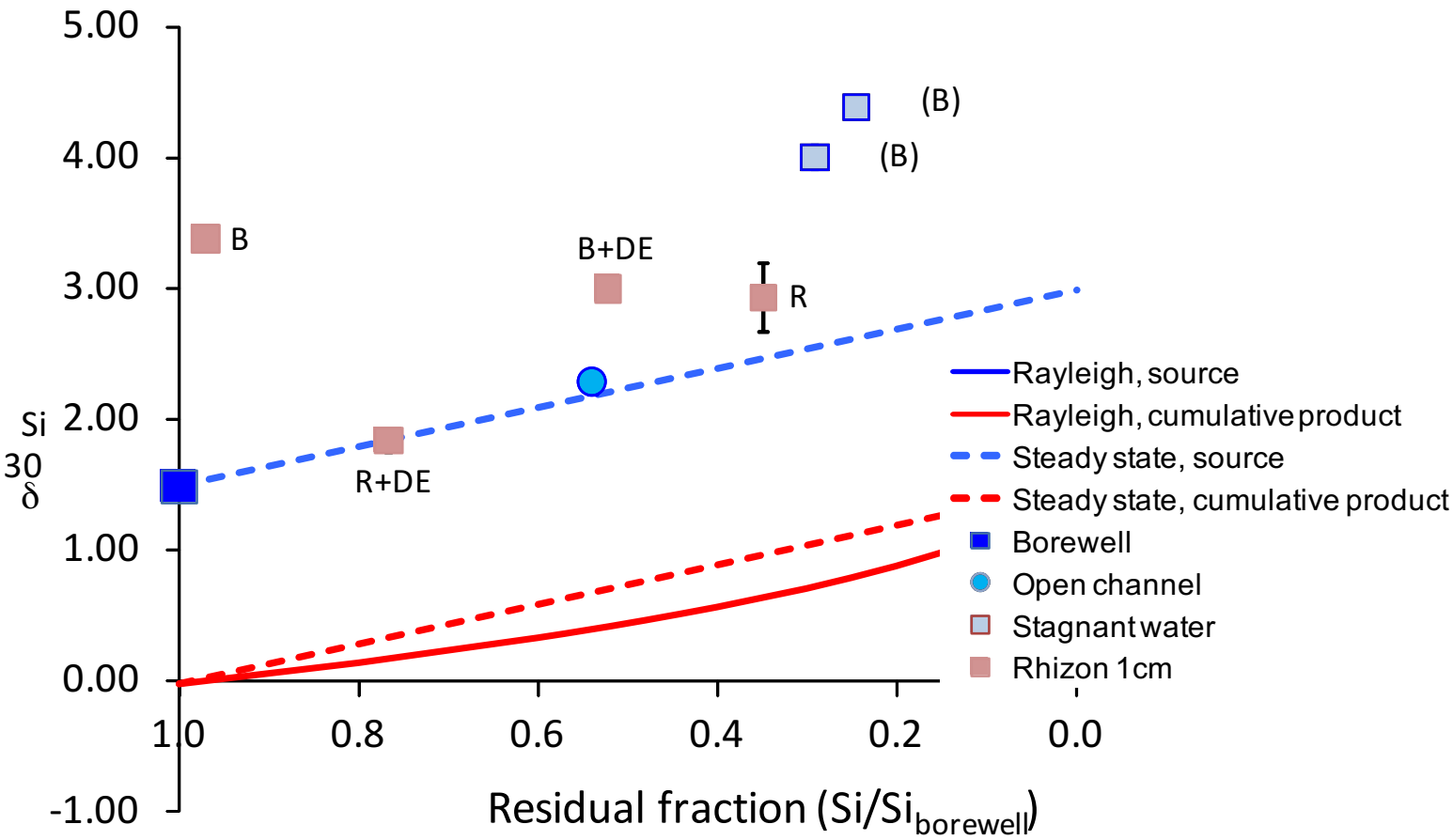
5.00
4.00
3.00
2.00
1.00
0.00
-1.00
Si
30
δ
(B)
(B)
B
B+DE
R
R+DE
1.0
0.8
0.6
0.4
0.2
0.0
Residual fraction (Si/Si borewell)
Rayleigh, source
Rayleigh, cumulative product
Steady state, source
Steady state, cumulative product
Borewell
Open channel
Stagnant water
Rhizon 1cm

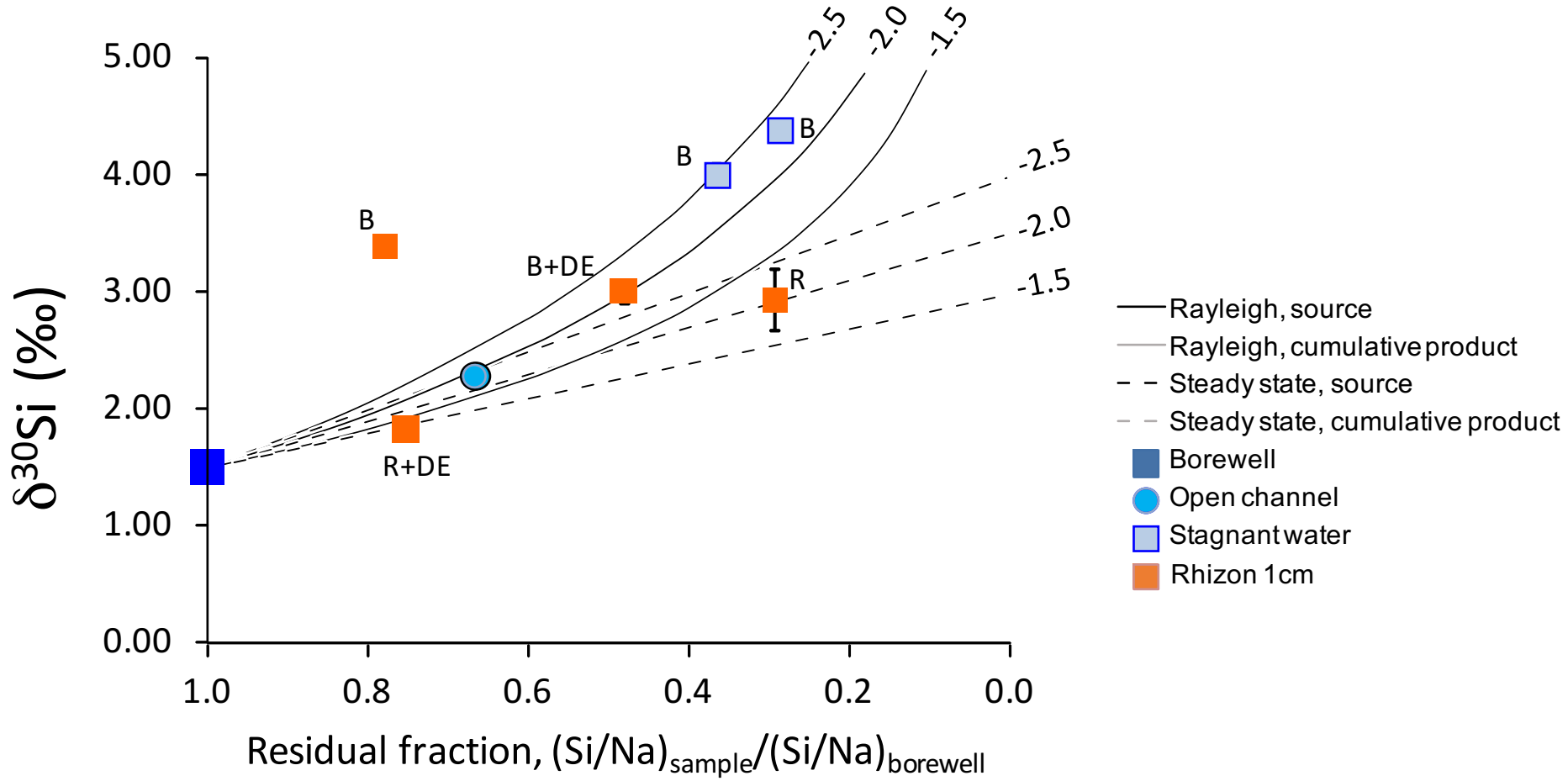
5.00
4.00
3.00
2.00
1.00
0.00
1.0
0.8
0.6
0.4
0.2
0.0
δ30Si (‰)
Residual fraction, (Si/Na)sample/(Si/Na)borewell
-2.5
-2.0
-1.5
B
B
B
B+DE
R
R+DE
-2.5
-2.0
-1.5
Rayleigh, source
Rayleigh, cumulative product
Steady state, source
Steady state, cumulative product
Borewell
Open channel
Stagnant water
Rhizon 1cm

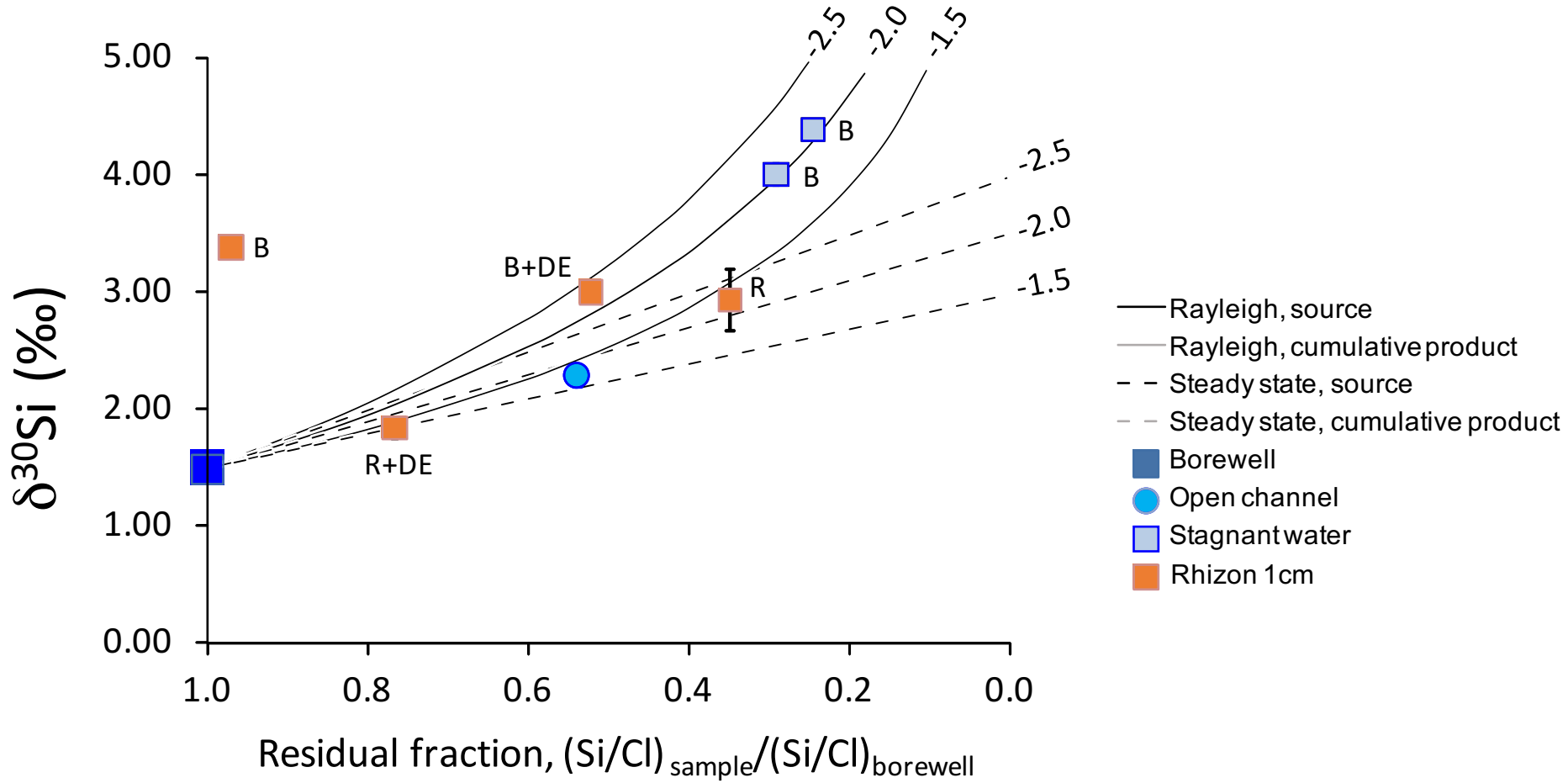
5.00
4.00
3.00
2.00
1.00
0.00
1.0
0.8
0.6
0.4
0.2
0.0
δ30Si (‰)
Residual fraction, (Si/Cl) sample/(Si/Cl)borewell
-2.5
-2.0
-1.5
-2.5
-2.0
-1.5
B
B
B
B+DE
R
R+DE
Rayleigh, source
Rayleigh, cumulative product
Steady state, source
Steady state, cumulative product
Borewell
Open channel
Stagnant water
Rhizon 1cm

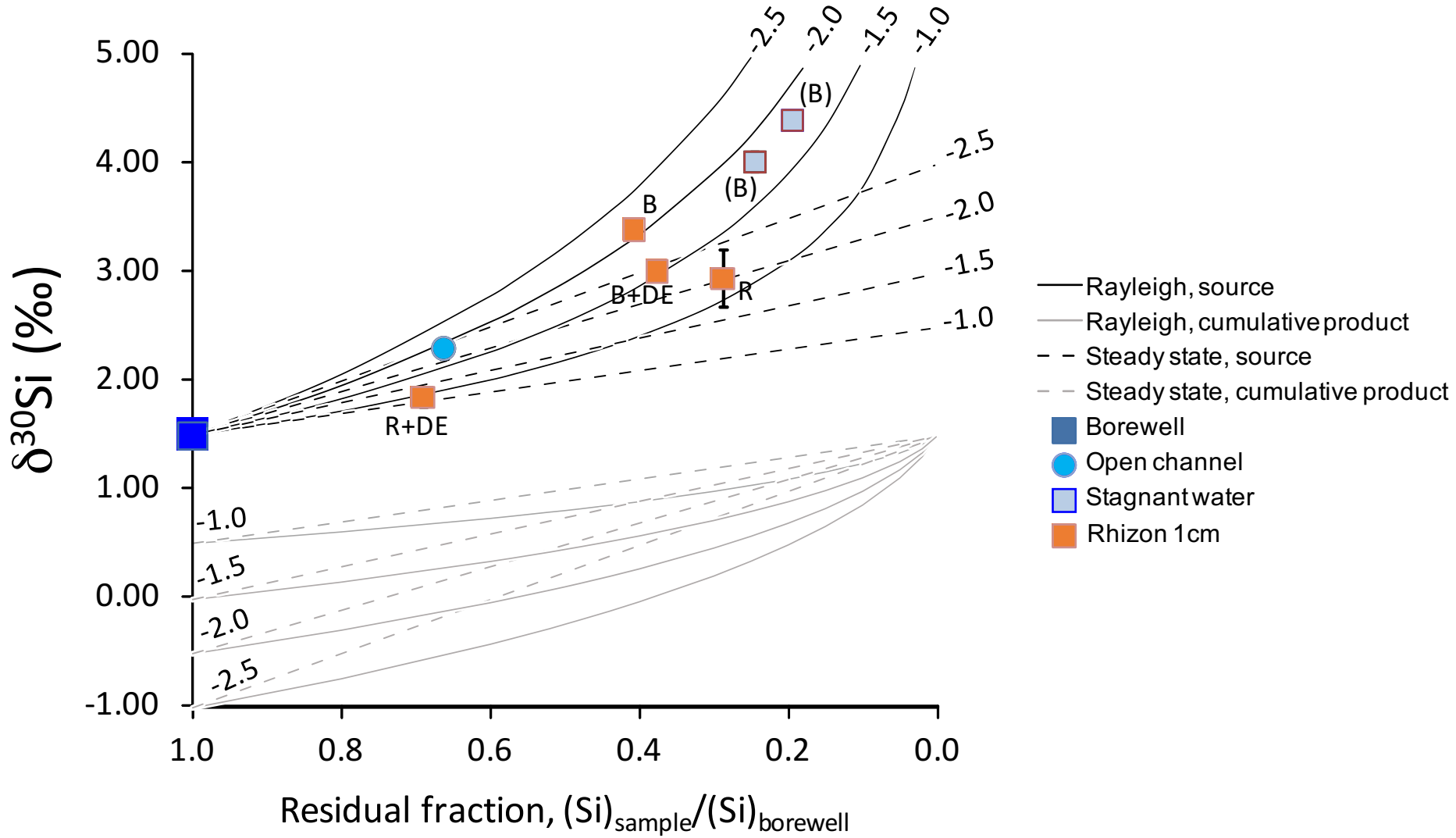
5.00
4.00
3.00
2.00
1.00
0.00
-1.00
1.0
0.8
0.6
0.4
0.2
0.0
δ30Si (‰)
Residual fraction, (Si)sample/(Si)borewell
-2.5
-2.0
-1.5
-1.0
(B)
(B)
B
B+DE
R
R+DE
-2.5
-2.0
-1.5
-1.0
-1.0
-1.5
-2.0
-2.5
Rayleigh, source
Rayleigh, cumulative product
Steady state, source
Steady state, cumulative product
Borewell
Open channel
Stagnant water
Rhizon 1cm

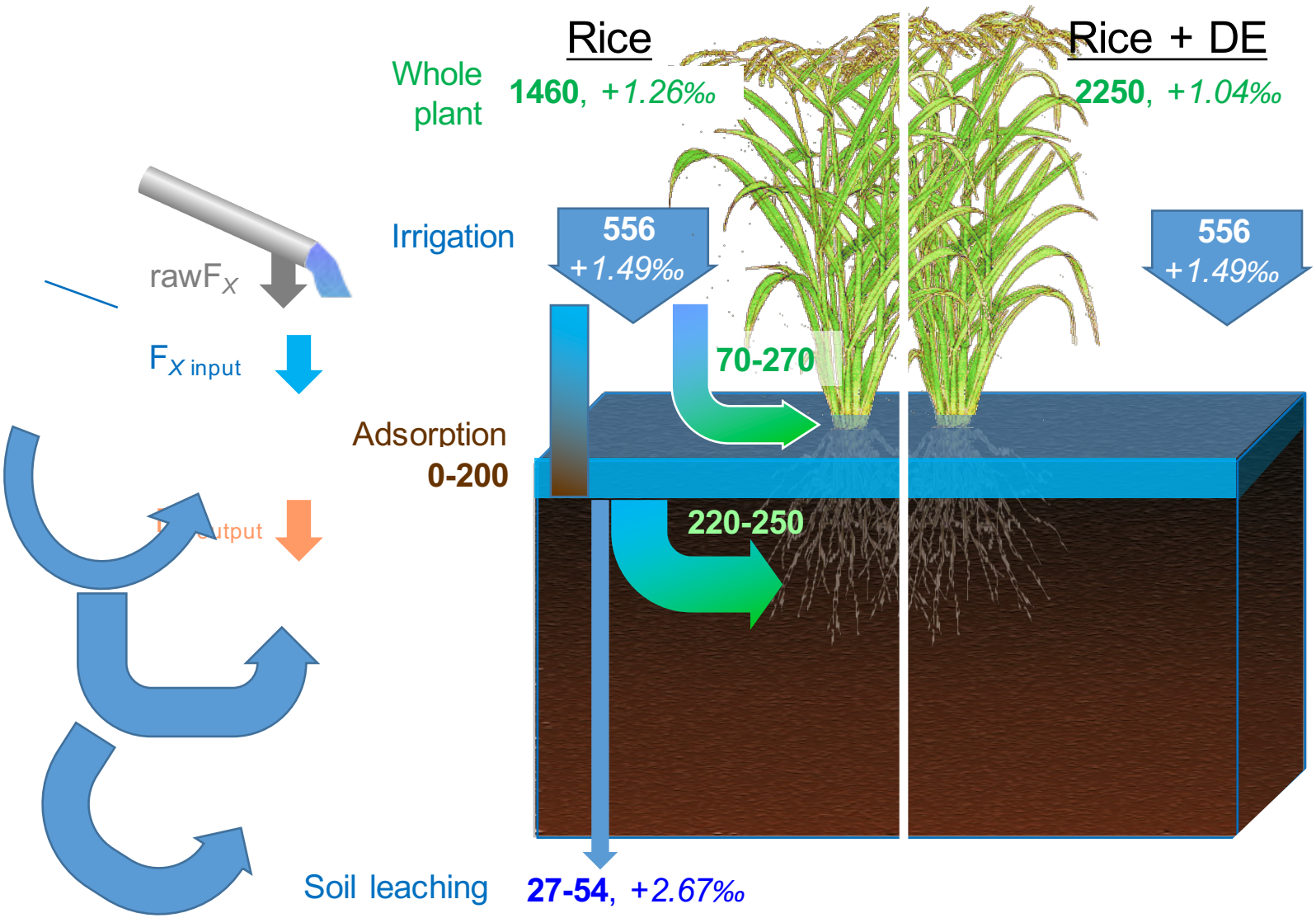
Rice
Rice + DE
Whole plant
1460, +1.26‰
2250, +1.04‰
rawF$_X$
F$_X$ input
Irrigation
556
+1.49‰
556
+1.49‰
70-270
Adsorption
0-200
220-250
Soil leaching
27-54, +2.67‰

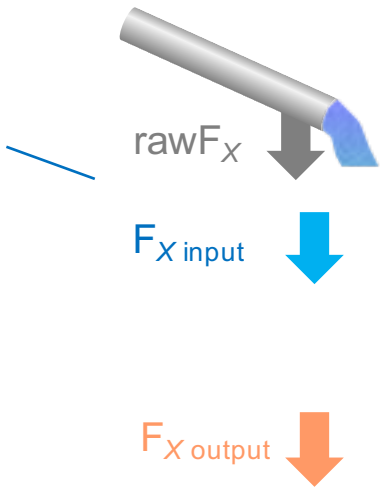
rawF$_X$
F$_X$ input
F$_X$ output

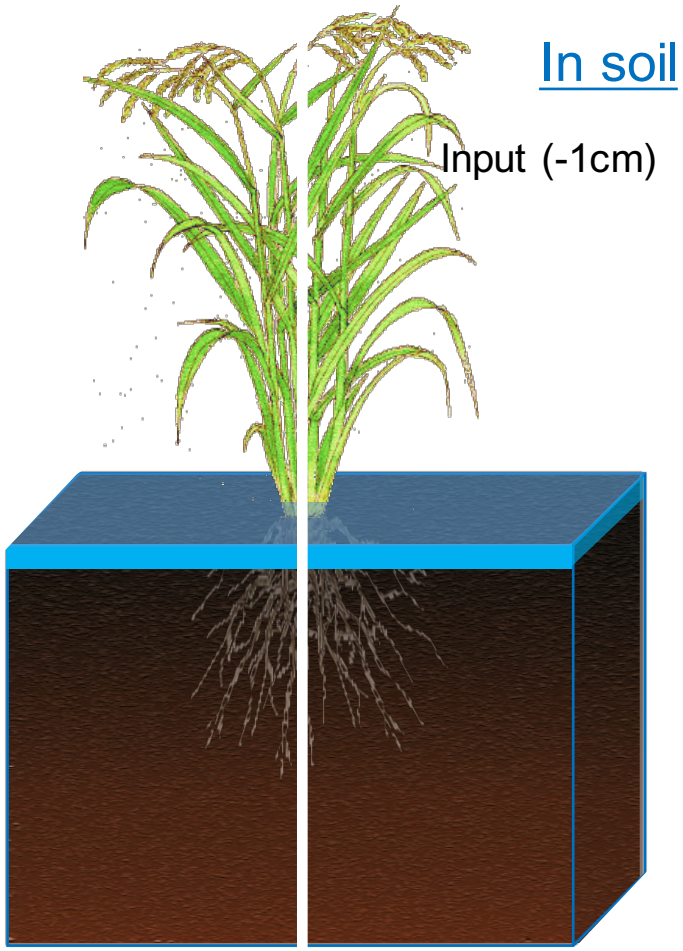
In soil
Input (-1cm)

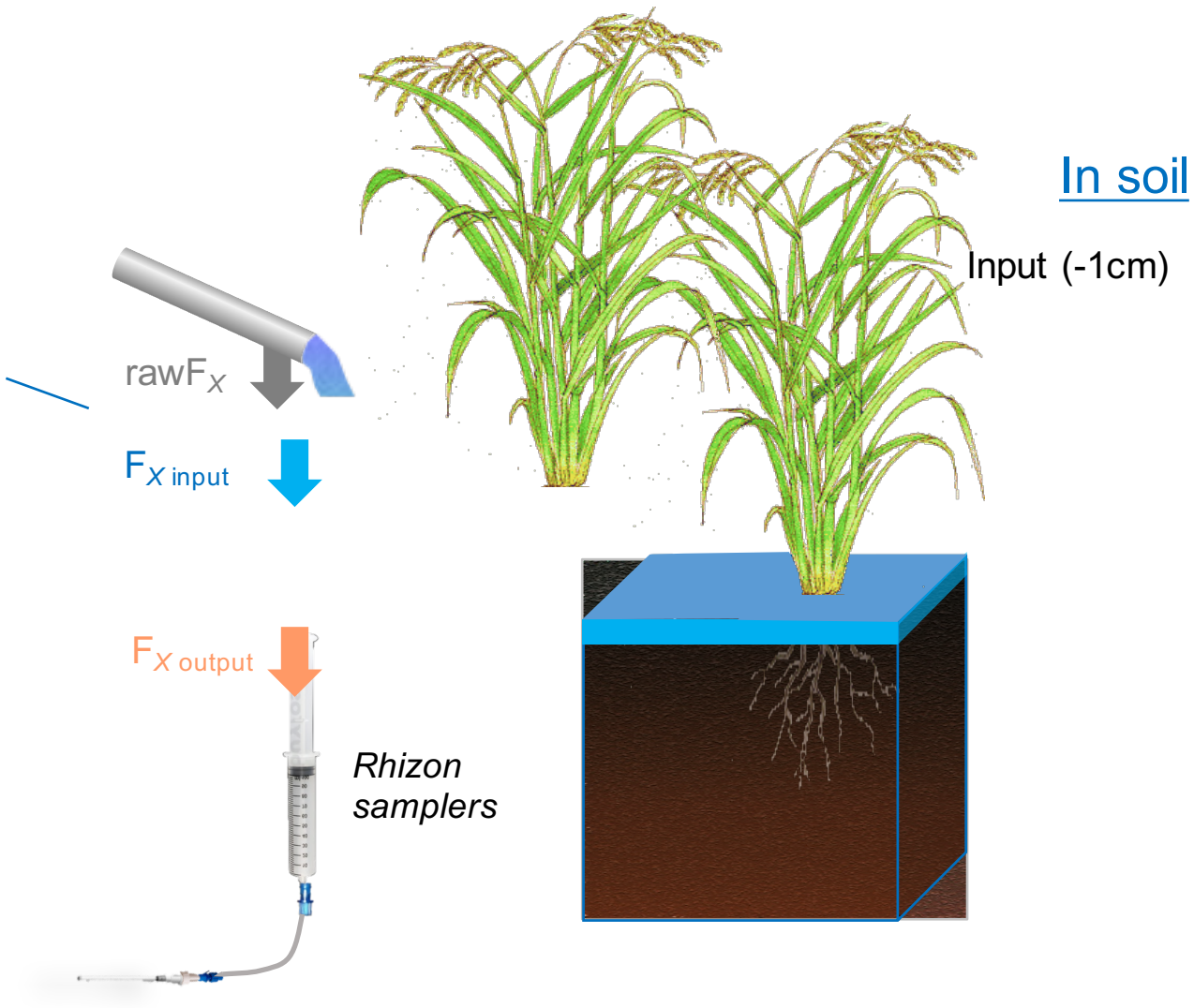
In soil
Input (-1cm)
rawF$_X$
F$_X$ input
F$_X$ output
Rhizon samplers

isotopic fractionation factor ($^{30}\varepsilon$) between bore well and stagnant water compositions is close to -1 ‰, i.e. the isotopic fractionation factor known for rice, indicating that above-ground DSi removal would be dominated by plant uptake upon adsorption. Within the soil layer, pore water DSi decreases much faster in rice experiments than in bare ones, demonstrating the efficiency of DSi rice uptake upon adsorption.

Total irrigation-DSi to plant-Si would then represent 24 to 36 % in rice experiments (over 1460 ± 270 mmol Si m^{-2} in biomass) and 15 to 23 % in rice+DE ones (over 2250 ± 180 mmol Si m^{-2}). The δ^{30}Si signature of whole plants was significantly different in the rice+DE plot analyzed, 0.99 ± 0.07 ‰, than in the rice one, 1.29 ± 0.07 ‰. According to these δ^{30}Si signatures, the main Si source from the soil would be the amorphous silica pool (ASi). A slight contribution of DE to the rice plant could be detected from the Si isotopic signature of rice.

Conclusions

The δ^{30}Si signatures of the various soil-plant compartments, when associated to Si mass balance at scale, constitute a reliable proxy of the Si behavior in paddy fields. The solute Si balance is controlled by rice uptake in rice plots and by adsorption and diatom uptake in bare ones. The main Si sources for the rice plants were soil ASi, irrigation Si and to a lesser extent Si fertilizer when it was applied.

Introduction

There is an increasing body of evidences showing that Si is playing a beneficial role for the development of crops (Guntzer et al., 2012; Liang et al., 2015). The Si concentration in plants depends primarily on the concentration of silicic acid in the soil solution (Ding et al. 2005; Henriet et al., 2008) and is not correlated to the total Si concentration of the soil (Brenchley and Maskell, 1927). However, correlations were observed between the Si concentration in rice and the percentage of clay in soils (Cheng, 1982), and between the Si concentration in rice or banana and the stock of weatherable minerals (Henriet et al., 2008; Makabe et al., 2009) but the contribution of the potential Si sources remain to be quantified. The geochemical cycle of Si in natural ecosystems such as forest and grassland is first controlled by silicate rock weathering which constitutes the primary source to hydro and ecosystems. Depending on weathering intensity, Si can be partitioned between a dissolved phase (DSi) and secondary clay minerals such as smectite (bisilialitisation, i.e. slight weathering) or kaolinite (monosialitisation, i.e. moderate to intense weathering), or dissolved congruently in case of

67 extreme weathering (allitisation) (e.g. Allen, 1997). The dissolved silica taken up by plants
68 precipitates as amorphous silica (ASi) particles called phytoliths (Piperno 1988; Meunier et
69 al., 2017). Because of its higher rate of dissolution in soil solution (Fraysse et al., 2009) Si
70 from phytoliths can be preferentially recycled by plants (Alexandre et al. 1997; Lucas, 2001)
71 or leached out of the soils and control the flux delivered to oceans by rivers as DSi and ASi
72 (Derry et al., 2005; Riotte et al., 2014; Cary et al., 2005; Hughes et al., 2011; Frings et al.,
73 2014).
74 The biogeochemical cycle of Si in cultivated land is poorly documented. According to
75 Vandevenne et al. (2012) agriculture may have disturbed the natural cycle of Si because plant
76 materials do not return to the field and are injected into the urban cycle. Several perturbations
77 have been documented in the surface soil horizons: depletion of the phytolith pool (Struyf et
78 al., 2010; Clymans et al., 2011; Guntzer et al., 2012; Vandevenne et al., 2015a) and a decrease
79 of crystallinity of clays (Irfan et al., 2017). Besides, repeated crop removal can reduce the
80 concentration of potentially available Si to the extent that Si fertilization is necessary (Datnoff
81 and Rodrigues, 2005; Meunier et al., 2008; Savant et al., 1997). Desplanques et al. (2006)
82 showed in a rice field of Camargue (France) that if soil ASi would be the only source of Si for
83 plants, this stock would be exhausted after five years of cultivation. Another potential cause
84 of Si-depletion in rice cropping systems is DSi leaching from the soil. According to the
85 estimation made by Nguyen et al, (2016) from an hydrological modelling in Viet-Nam, the
86 potential loss could reach 10 tons Si ha^{-1} yr^{-1} (350.10^3 mol Si ha^{-1} yr^{-1}), i.e. ten times the Si
87 taken up by rice plants in this system. Therefore, there is a need for better documenting the Si
88 budget in the cultivated land. In a recent rice cropping experiment in California where straw
89 was incorporated into the soil prior to cultivation, Seyffert et al. (2013) monitored the Ge/Si
90 ratio in soil pore water and observed an increase of Ge/Si during the fallow season and a
91 decrease during the cropping season. These authors assigned these relative variations to the Si
92 release from the straw and its further uptake by the rice crop. Improving the quantification of
93 Si-fertilizer's contribution for adjusting the doses applied to the plant requirements would
94 require not only a thorough Si mass balance in paddy fields (quantifying the Si sources and
95 sinks of Si, including Si-fertilizers contribution), but also a proxy of Si sources.
96
97 Studying the silicon isotopic compositions of the various soil-water-plant compartments of
98 rice cropping experiments could bring new insight for the Si mass balance at soil-plant scale
99 and particularly about the nature of the Si sources to the rice. Silicon has three natural (stable)
100 isotopes, ^{28}Si, ^{29}Si, ^{30}Si which fractionate during water-soil interactions and plant uptake

(reviews in Opfergelt et al., 2012; Frings et al., 2016). The partition of Si between dissolved load and clay minerals during silicate weathering induces preferential allocation of the light Si isotopes in clay minerals and subsequent enrichment of heavy Si isotopes in the solution (Ziegler et al., 2005; Georg et al., 2007). As a consequence, primary bedrock silicates, secondary clay minerals and soil pore water often exhibit distinct isotopic signatures. Similarly, Si adsorption onto ferrihydrite or goethite favors light isotopes (Delstanche et al., 2009) according to an isotopic fractionation factor ($^{30}\varepsilon$) varying between -1.1 ‰ for ferrihydrite to -1.6 ‰ for goethite. Such isotopic fractionation also occur between plant and solution. The first studies of the Si isotopic signatures in rice plants highlighted a $^{30}\varepsilon$ between the soil or the hydroponic solution and the rice plants of -1 ‰ (Ding et al., 2008), a value similar to the few other plants measured up to now: banana, wheat or bamboo (Opfergelt et al., 2012 and references therein). Recently, hydroponic experiments (Sun et al., 2016) revealed that the Si isotopic fractionation factor between the external solution and the whole plant could indeed range from -0.4 ‰ to -1.13 ‰ according to the DSi concentration of the solution (here 0.17 to 8.5 mmol Si L^{-1}). Sun et al. deduce from these experiments that the rice plant takes up most of the silica through an active mechanism and that the preferential uptake of light Si isotopes occurs via a passive mechanism. The respective δ^{30}Si signatures of rice and feeding solution are then expected to clarify the Si accumulation processes in the plant. To our knowledge, the only study which reported Si isotopes on cultivated soils solution showed a shift to heavier values, attributed to a decrease of the phytolith source for DSi (Vandevenne et al., 2015b).

The objective of this study is to perform a rice cropping experiment for identifying and assessing the contributions of the various Si sources to the plant and the possible contribution of a Si-fertilizer, diatomaceous earth (DE). DE have proven to be a good fertilizer in India as measured by the increased Si concentration in the shoots and the grain yield (Crooks and Prentice, 2016; Pati et al., 2016). Indeed, DE contains relics of diatom tests that are made of amorphous silica. Amorphous silica particles (phytoliths and diatoms) are highly soluble compared to the other soil silicates minerals around neutral pH (Fraysse et al., 2009). We combined a solute budget at soil-plant scale for estimating the contribution of irrigation with the Si isotopic compositions (δ^{30}Si) of the various soil, plant and water compartments for assessing the complementary Si sources. In order to decipher the plant-driven processes from the water-soil interactions, the solute budget was performed in four different conditions: bare plot, bare plot with addition of DE, rice plot and rice plot with DE addition.

1 Materials and methods

1.1 Experimental set up

The study took place at the VC Farm (Experimental farm of Mandya, Southern India which depends on the University of Agricultural Sciences, Bengaluru, 12°34'22"N, 76°49'38.5"E). The soil is categorized as Typic Rhodustalfs, has a sandy loam texture, a pH of 7.1 and contains quartz, feldspar, goethite, kaolinite and illite clay minerals (see also Sandhya K. 2016 for further information for the soil composition). A paddy field was divided into 16 plots of 4 by 5m ($20m^2$), isolated from each other by furrows (Fig. 1) to prevent any drainage input/output from adjacent plot.

Each plot was inundated and ploughed. Then, four different experiments were set up, each with four replicates: (1) barren soil (further referred as "bare"), (2) barren soil with application of 30 g m^{-2} of diatom earth from Agripower Australia Ltd. (DE; further referred as "bare+DE") (3) planted with rice (further referred as "rice"), and (4) rice planted with application of 30 g m^{-2} of DE before planting (further referred as "rice+DE"). In rice and rice+DE plots, twenty one days old rice seedlings of species KMP-101, locally called Thanu, were transplanted with a spacing of 20 cm by 10 cm. The total fertilizer applied was 27.2 g m^{-2} of urea (CH_4N_2O), 39 g m^{-2} of single superphosphate (SSP, $Ca(H_2PO_4)_2$) and 10.4 g m^{-2} of muriate of potash (MOP, KCl), corresponding respectively to 910 mmol N m^{-2}, 248 mmol P m^{-2} and 140 mmol K m^{-2}. The entire dose of SSP, half dose of MOP and urea were applied prior to transplanting. Remaining MOP and urea were given as two splits at 30th and 60th days after transplanting. All plots were irrigated once in a week with the local borewell water for the 100 days duration of the experiment (22nd August to 16th December 2015). The applied DE (Agripower Australia Ltd) contains amorphous silica particles (diatom frustules) and crystalline minerals (quartz, smectite, kaolinite).

1.2 Water and plant sampling

Water from the bore well used for irrigation was collected four times from March 2015 to November 2016 for checking the stability of its chemical composition. Two soil pore water samplers (Rhizon®) were installed in the center of each plot: one just below soil surface at 1 cm depth to collect infiltration water (considered as soil water input), the other at 40 cm depth to collect soil leaching (considered as soil output water). Samplers at 40 cm were installed prior to ploughing and their connection tube buried. To avoid disturbance of local

soil properties, particularly preferential infiltration, connection tube was unearthed the day of transplanting, after ploughing. Shallow Rhizon samplers were inserted horizontally after transplanting. Soil pore waters were collected twice in a month (n=6-9 per plot, 33 to 36 samples per experiment) by suction with a 50 ml syringe and stored in polypropylene bottles. Volume collected each time ranged from few ml to 50 ml. Unfortunately, we observed from chemical analyses that Rhizon samplers at 40 cm were collecting the local shallow groundwater, which composition is very close to the canal irrigation water used in the command area of the KRS dam (Meunier et al., 2015), instead of collecting soil leaching. As an alternative, four plots (one per experiment) were cored up to 20 cm depth to sample soil pore water not impacted by the local groundwater in November 2015, i.e. about one month before harvest. Cores were sliced in five sections (0-2.5 cm, 2.5-5 cm, 5-10 cm, 10-15 cm and 15-20 cm) and soil pore water extracted by centrifugation and/or hydraulic press when pore water content was too low for extraction by centrifugation. Few additional samples of stagnant water, from a previous experiment were also analyzed for comparison with Rhizon and core samples. Water chemistry was determined at the Indo-French Cell for Water Sciences, Indian Institute of Sciences, Bengaluru. Major anions and cations were analysed with an ion chromatograph (Metrohm) and silica using the molybdate blue method and a UV-visible Knauer detector. The overall precision obtained for the concentration measurements was better than 10%. The reference materials used for the quality check was ION 96.4 and PERADE (Environment Canada). Plant biomass was harvested at plant maturity and weighed. Straw (leaves and stems) and grains with husk were dried and preserved for further chemical and isotopic analyses. Finally, one algal mat per experiment was collected to assess the presence of diatoms and check the isotopic composition of ground-surface soil ASi.

All of the data were analyzed statistically using one-way ANOVA with XLSTAT (Addinsoft) at a significance level of $P < 0.05$ via the Tukey test.

1.3 Determination of plant Si and soil ASi

Si concentration in plants was measured following the method described in Ma and Takahashi (2002). Briefly the rice plants were washed in distilled water before oven dried at 70°C for 2-3h and finely grounded. Samples were digested in concentrated HNO_3, H_2O_2 and HF using a microwave digestion system before dilution in 4% boric acid. The Si was determined using the molybdenum blue method at 600nm. The ASi soil pool was separated from the soil matrix (5g aliquot) using heavy liquid flotation. Carbonates were first removed with HCl (at 37 %

overnight), then the organic matter (OM) was oxidized with H_2O_2 33 % at 50–70 °C. The clay fraction was removed by decantation with sodium hexametaphosphate to ease deflocculation and the heavy minerals by flotation using $ZnBr_2$ dense liquor set at d=2.3 g cm^{-3}. ASi_{zb} fraction should theoretically be composed of pure amorphous silica. However, this fraction may contain some impurities, typically clays, which could impact the estimation of ASi stock in soil and also alter the $\delta^{30}Si$ signature of phytoliths. In order to assess the purity of ASi_{zb} samples and to correct if necessary ASi_{zb} and $\delta^{30}Si$ values, we used an index based on the chemical composition of ASi_{zb} fraction that considers Al as a proxy of clay contamination (kaolinite or smectite) according to the equation:

$$ASi_{zb}\ purity = (Si - Al) / Si \qquad (1)$$

With Si and Al contents in mol kg^{-1}. The ASi_{zb} purity of pure silica fraction should be one, pure kaolinite zero and Ca-smectite around 0.58. The concentration of Si from ASi can be calculated considering a mean water content in opal of 10 % (Bartoli & Wilding, 1980) equivalent to 0.37 moles of H_2O for 2 moles of SiO_2 and the purity index following the equation:

$$ASi = ASi_{zb} \,.\, ASi_{zb}\ purity \,.\, 0.42 \qquad (2)$$

With 0.42 the conversion factor from opal to Si.

1.4 Solute mass balance at soil-plant scale

The objective of solute Si mass balance at soil-plant scale is to assess where and how much dissolved silica (DSi) is removed from the system, which first requires a water budget. The total input water flux (Q_{total}) is composed of irrigation and rainfall. Irrigation flux (I) was quantified by measuring the yield of the borewell pump and by irrigating all plots for a same known duration. Rainfall (R) was measured with the manual rain gauge of the VFS farm. Estimation of the DSi flux leached from the soil requires estimating the leaching water flux ($Q_{soil\ output}$) which depends on the intensity of local evapotranspiration (ET). $Q_{soil\ output}$ was assessed following two ways:

(1) Considering a simplified water balance. In absence of runoff, $Q_{soil\ output}$ can be deduced from the relation $Q_{soil\ output} \approx Q_{total} - ET = R + I - ET$. In bare soil conditions, ET is expected to be similar to the potential evapotranspiration (PET). In paddy fields, the

actual evapotranspiration (ET_a) is known to exceed PET. For this reason, ET_a is usually estimated by multiplying PET with a crop coefficient. Crop coefficient varies according to the local climatic conditions and along the cropping season. For the simplified water balance, we used the value of 1.15, corresponding to the average crop coefficient of rice for semi-arid and moderate wind conditions, provided by FAO (Allen et al., 1998). This value is consistent with the estimates of Tyagi et al. (2000) in Northern India and more recently of Reddy et al. (2015) in Southern India. The local PET was assessed from solar radiation and temperature data for the 100 days of cropping period (data from the Karnataka State Natural Disaster Monitoring Centre, KSNDMC). This $Q_{soil\ output}$ estimation is independent from chemical data.

(2) Using the solute mass balance of a conservative element. It relies on the hypothesis that the soil input flux of a conservative element is equal to the soil output flux (steady state hypothesis). A conservative behavior means that interactions with soil and plant are limited enough to be neglected and then, that its concentration in the soil layer only depends on the evapotranspiration intensity. This approach, classically used for estimating groundwater recharge in pristine watershed (e.g. Maréchal et al., 2009, 2011a,b; Fouépé et al., 2011), considers chloride as the conservative element and is then known as the chloride mass balance method (CMB). In most cases Cl is considered to originate only from atmospheric inputs. However, CMB was also applied with success in anthropic systems like urban watersheds (Fouépé Takounjou et al., 2011) or agriculture in a context similar to this study: a winter wheat plot fertilized with KCl for three decades (Tyner et al., 2000). Since in the present study it was not possible to monitor the soil pore water composition at 40 cm depth, CMB was applied for the first 20 cm of soil using the core pore water composition with, as main advantage, being able to assess the above-ground evaporation and to track, once in the soil, the progressive enrichment of Cl with depth by transpiration and compare it with the expected depletion of silica. The small scale CMB provides the opportunity to test the pertinence of sodium as conservative element, since Na is not brought by fertilizers nor involved in plant cycle. Above-ground evaporation was assessed for all four experiments by comparing the average Cl or Na concentration in Q_{total} with the average Cl or Na concentration in the infiltrating solution (1 cm depth Rhizon sampler) according to the relationship:

$$Q_{AG\ evaporation} = Q_{total} - \frac{\overline{[Na,Cl]_{borewell}}.I + \overline{[Na,Cl]_{rain}}.R}{[Na,Cl]_{surface\ porewater}} \quad (3)$$

With $\overline{[Na,Cl]_{borewell}}$ the average Na or Cl concentration in irrigation water (n=6), $\overline{[Na,Cl]_{rain}}$ the average Na or Cl concentration in rain water, here taken from long term monitoring of the Mule Hole watershed (n ≈ 200; Riotte et al., 2014), and $\overline{[Na,Cl]_{surface\ porewater}}$ the average Na or Cl concentration in the 1cm depth pore water collected with Rhizon sampler (n=8 to 9 per plot, 4 plots per experiment, then 32 to 36 samples per experiment). Water fluxes are specific, which means they are expressed per surface unit in mm or L/m^2. The water flux infiltrating in the soil can be deduced as:

$$Q_{input} = Q_{total} - Q_{AG\ evaporation} \quad (4)$$

The specific water flux leached from the soil, Q_{output}, can be approximated for each experiment by simple mass balance, assuming that the soil input flux of the conservative element is equal to the soil output flux, which is the principle of the CMB method. Here, to be consistent with the soil output composition (core pore water at 15-20 cm), the soil input composition considered for the calculation was the shallowest core pore water (0-2.5 cm) of each experiment. Then, Q_{output} can be described as:

$$Q_{output} = Q_{input} . \frac{[Na,Cl]_{0-2.5cm\ porewater}}{[Na,Cl]_{15-20cm\ porewater}} \quad (5)$$

Soil input and output DSi fluxes (FSi_{input} and FSi_{output}, respectively) were estimated in a second step, by multiplying DSi concentrations in 1 cm and 15-20 cm pore waters, respectively, with the water fluxes estimated from ET or CMB approaches. The difference between input and output DSi fluxes (ΔFSi) provides an estimate of the apparent removal or addition DSi flux. This flux is considered as "apparent" because it may not account for the entire Si flux mobilized or removed from the soil pore water. However, the $\delta^{30}Si$ signature of this flux is expected to provide constrains on the water-soil-(plant) processes involved in the soil. It can be assessed according to a simple isotopic mass balance equation:

$$\delta^{30}Si_{\Delta FSi} = \frac{FSi_{output}.\delta^{30}Si_{output} - FSi_{input}.\delta^{30}Si_{input}}{\Delta FSi} \quad (6)$$

1.5 δ^{30}Si measurements

The δ^{30}Si signatures were determined on irrigation water, stagnant water (n=3), shallow (1 cm) Rhizon pore water (n=4), core pore water depth profiles (n=25) and on solid silica pools, i.e. DE, clay fraction, ASi of algal mats (n=4), ASi of soils (n=2) straw (n=2) and - rice grains with husk (n=2). Solid samples were first digested by alkaline fusion with NaOH and dissolved in water and diluted HCl, following the procedure of Zambardi and Poitrasson (2011) modified from Georg et al. (2006). Both digested solid and dissolved samples were processes through Bio-Rad AG50-X12 ion exchange resin to remove the cationic matrix and elute the silica fraction. This latter was diluted to 2 mg L^{-1}. Then, 1 mg L^{-1} of Mg was added as internal standard for online correction of mass bias during the analysis.

Isotopic measurements were performed on a Multi-Collector ICP-MS Neptune (Thermo®) at medium resolution and replicated 3 times. The reference material NBS 28, also spiked with 1 mg L^{-1} of Mg, was measured between each sample (bracketing mode). Isotopic data were normalized to the NBS 28 international standard and expressed in per mil (‰) following the relation:

$$\delta^{30}Si\ (‰) = \left(\frac{\left(\frac{^{30}Si}{^{28}Si}\right)_{sample}}{\left(\frac{^{30}Si}{^{28}Si}\right)_{NBS\ 28}} - 1 \right) . 1000$$

The uncertainty associated with the δ^{30}Si data (2σ) corresponds to the relative standard deviation obtained from the 3 replicates. The reproducibility was checked by regular measurements of the reference material BHVO (a basaltic rock). The average δ^{30}Si obtained from 2010 to 2016 measurements, -0.27 ± 0.06 ‰ (n=24), matches the values obtained by Zambardi and Poitrasson (2011), -0.27 ± 0.08 ‰ and Savage et al. (2012), -0.30 ± 0.09 ‰. The standard deviation found for BHVO measurements (±0.06 ‰) will be considered as the minimum precision of δ^{30}Si data.

2 Results

2.1 Chemical composition of waters

The composition of the borewell water was stable over the whole study period, Cl and Na concentrations (3484 ± 383 µmol L^{-1}; 6215 ± 360 µmol L^{-1}, Table 1) being within the range found in the region for groundwater located in semi-arid conditions and impacted by agriculture (Siva Soumya et al., 2013). Borewell water is also particularly rich in DSi, on average 1217 ± 155 µmol L^{-1}, as compared for instance to the Kaveri river, between 100 and 300 µmol L^{-1} (Meunier et al., 2015) or to the groundwater of a nearby forested watershed (Maréchal et al., 2011b). Such concentration should make irrigation water a significant Si source to plants. Sodium and Chloride concentrations of shallow Rhizon pore waters (n=138) and stagnant water (n=2) stretch on a linear relationship ($R^2 = 0.83$ for all samples, $0.72 < R^2 < 0.93$ for the 16 individual plots), on which the borewell composition falls too. This trend reflects the common dilution (by rain) and concentration (by evaporation) cycles of both elements (Fig. 2a). On the contrary, DSi concentrations are always more diluted than the borewell, even at the highest Na concentrations. DSi ranges from 100 µmol L^{-1} (Fig. 2b), which correspond to the equilibrium with quartz, to 1000 µmol L^{-1}.

DSi concentrations in rice and rice+DE experiments are on average lower than in bare and bare+DE ones. Within the soil, the Cl and Na concentrations of core pore water samples increase with depth (Table 2, figure 3). DSi exhibits again a different pattern with sharp decrease to ~100 µmol L^{-1} within the upper five centimeters in rice and rice+DE plots, and more regular decrease in bare and bare+DE plots (Fig. 3). Between 15 and 20 cm depth, DSi concentration of rice plots cannot be distinguished from those of bare plots.

2.2 Water and solute mass balance

The total amount of water received by each plot over the cultivation period (from transplantation to harvest) was 889 mm, comprising 473 mm from bore well and 416 mm from rainfall. Considering a PET of 433 mm for this period and a crop coefficient for rice of 1.15 (Allen et al., 1998), the actual evapotranspiration in rice plots should be 500 mm. In absence of surface runoff or lateral subsurface flow, the soil leaching flux would be 390 mm beneath rice plots, while it would be slightly higher, 455 mm, in bare soils.

Using equations of section 2.4 and either Na or Cl as conservative element, it was possible to distinguish the water and solute budgets both above-ground (in stagnant water, before infiltration) and below-ground (within soil). Above-ground evapotranspiration (Eq. 3) ranges from 370 mm in bare experiment to 410 mm in rice+DE experiment (Table 3). No difference was observed between Cl- and Na-based calculations. Both estimations agree with direct pan measurements made by Siva Sivapalan (2015) in similar climatic conditions and latitude. Water fluxes leached from the soil layer were assessed using Cl and Na concentrations measured in the deepest soil pore waters and Eq. 5. Sodium-based calculations provided homogeneous leaching water fluxes across experiments, from 180 mm (rice + DE) to 230 mm (rice), i.e. twice lower than those estimated from the water balance, while chloride-based leaching water fluxes were more scattered and ranged from 110 (rice + DE) to 460 mm (rice). Since DSi of stagnant water fluctuates over time due to concentration by evaporation or dilution by rain (Figure 2b), deducing the DSi flux removed at the ground surface from the average DSi concentration only would provide a value marred by a large uncertainty. Normalizing DSi to Na or Cl allows overcoming dilution and concentrations effects and then improving the precision associated to calculation of DSi removal. Average Si/Na molar ratios a 1cm depth of bare and bare+DE experiments are 0.128 and 0.124, respectively, while they are slightly but significantly lower in rice and rice+DE experiments, 0.095 and 0.092, respectively according to the Tukey HSD test (Table 1). Standards deviations are about twice larger for Si/Cl, probably because of KCl additions, but remained narrower compared to the DSi fluctuations. The above-ground DSi removal calculated from Na/Si ratios was 210 $mmol.m^{-2}$ in bare and bare+DE experiments, and 275-280 $mmolSi\ m^{-2}$ in rice and rice+DE experiments. Similar values were obtained using Si/Cl (Table 3). These results indicate that less than two third of the DSi flux brought by borewell irrigation to bare experiments and about half of DSi in rice experiments infiltrate into the ground; such proportion of above-ground DSi removal was unexpected and has, to our knowledge, never been reported before. By difference with the input DSi flux to each plot, the DSi flux infiltrating into the soil would be 410 $mmolSi\ m^{-2}$ in bare and bare+DE experiments and 320 $mmolSi\ m^{-2}$ in rice and rice+DE experiments. Soil leaching DSi fluxes, calculated using the deepest soil pore water compositions and leaching water fluxes, ranged from 27 to 55 $mmolSi\ m^{-2}$ in rice experiment to 40 to 84 $mmolSi\ m^{-2}$ in bare+DE experiment. This value is relatively low compared to the Si percolating flux calculated in humid tropical conditions (Philippines; Klotzbücher et al., 2015), because of the high percolating water flux. The DSi removal within the soil layer,

388 calculated as the difference between soil DSi input and leaching fluxes, was slightly lower in
389 rice experiments (190 to 235 mmolSi m^{-2}) than in bare ones (250 to 310 mmolSi m^{-2}).
390

391 ### *2.3 δ^{30}Si of waters*

392 The δ^{30}Si of the bore-well water, 1.49 ‰, falls in the upper part of the range observed up to
393 now in groundwater (Frings et al., 2016), but it is similar to the values found in the
394 groundwater of the Mule Hole watershed (0.81 to 1.49 ‰) located on the same peninsular
395 gneissic complex as Mandya. This signature evolves towards heavy values, up to 4.39 ‰, as
396 water stagnates and DSi drops. With the exception of one sample which exhibits a low δ^{30}Si
397 value (1.89 ‰) associated to high DSi (849 µmol L^{-1}), shallow (1 cm) soil pore water display
398 heavy δ^{30}Si ranging from 2.94 to 4.36 ‰ (Fig. 3). These signature slightly decrease with
399 depth, down to 2.04 to 3.26 ‰ at 15-20 cm. The δ^{30}Si of these soil pore water are
400 significantly heavier than those ever measured up to now (see review of Frings et al., 2016).
401 On average, δ^{30}Si of soil pore water is slightly lower in rice plots than in bare plots, but all
402 pore waters evolve with depth within the same δ^{30}Si range, whatever the experiment.
403

404 ### *2.4 Soil silica pools and δ^{30}Si*

405 The soils of the sub-humid and semi-arid zones of the Deccan plateau are known to be
406 immature and still contain primary minerals like plagioclases and quartz (e.g. Braun et al.,
407 2009). In Mandya, the <2 µm fraction of the soil, which includes clays *sensus stricto* and clay
408 minerals like Fe-oxyhydroxides, accounts for only 21 % which means that primary minerals
409 and ASi compose about 80% of the soil. The soil ASi_{ZB} fractions in rice and rice+DE plots,
410 when corrected from impurities, are 1.9 and 1.8 % (Table 4). Such ASi values are twice
411 higher than in the Mule Hole forest, located in similar geological settings (~1%), or than in
412 some other paddy fields (Desplanques et al., 2006). Taking into account the ASi_{ZB} fraction,
413 the proportion of Si located in primary silicates would be at least 75%.
414 The δ^{30}Si of primary minerals can be assimilated to the whole bedrock signature (-0.34 ‰)
415 determined for the Mule Hole watershed. Soil clays of Mandya display δ^{30}Si of -
416 1.09 ± 0.06 ‰, slightly heavier but close to the Mule Hole Ferralsol clays (-1.3 ± 0.15 ‰).
417 This confirms that the fractionation factor ($^{30}\varepsilon$) between bedrock and clay in this weathering
418 context is lower than that predicted by models (Meheut et al., 2007) or measured in tropical
419 (Ziegler et al., 2005) or boreal (Georg et al., 2007) soils. The slightly heavier δ^{30}Si in

Mandya's clay could however be explained by a minor contribution of silica adsorbed onto ferrihydrite in the clay-size fraction, since the granulometric fraction recovered contained more Fe than Si (Table 4). The $\delta^{30}Si$ of soil ASi_{ZB} fractions were corrected, when needed, from clay contribution using the purity index described in section 2.3. Correction consists in extrapolating the mixing curve between clay and ASi to a purity index of 1 (Fig. 4). Both ASi_{ZB} compositions align on the same mixing curve which tends towards $\delta^{30}Si$ of 0.5 ‰.

2.5 ASi stock and $\delta^{30}Si$ of rice plants, algal mats and DE

The rice biomass, Si content in rice and its $\delta^{30}Si$ signature are presented in Table 5. Because root Si accounts for only few percent of the total Si taken up by rice plants (Ding et al., 2005; Sun et al., 2008), straw (stem and leaves) and whole grain (grain and husk) represent the bulk rice Si uptake. Average straw biomass and grain weights harvested in the four rice plots are 7.96 ± 0.60 tons ha^{-1} and 6.12 ± 0.26 tons ha^{-1}, respectively. In the rice+DE plots, straw biomass is significantly higher, 10.3 ± 0.5 tons ha^{-1}, for a similar whole grain (grain + husk) yield as rice experiments, 6.33±0.71 tons ha^{-1}. Average straw Si contents in rice and rice+DE experiments are comparable, 4.72 ± 0.72 % and 5.77 ± 0.30 %, respectively. These values fall in the upper side of the range found in China by Ding et al. (2005) but are twice higher than in Camargue (South of France; Desplanques et al., 2006). Whole grain Si contents (including husk), 0.55 ± 0.09 and 0.59 ± 0.04 %, respectively, are also similar to the husk and grain values of Ding et al. (2005) and Sun et al. (2008). The average Si uptake in rice experiments, deduced from biomass and ASi data, are 377 ± 81 kg ha^{-1} (1.34 ± 0.29 molSi m^{-2}) in straw and 33.3 ± 6.3 kg ha^{-1} (0.12 ± 0.02 molSi m^{-2}) in grains, comparable to Desplanques et al. (2006) and in rice+DE experiments 595 ± 54 kg ha^{-1} (2.12 ± 0.19 molSi m^{-2}) in straw and 37.5 ± 4.5 kg ha^{-1} (0.13 ± 0.02 molSi m^{-2}) in grains. The Si uptake by the whole plants is then significantly higher in rice+DE experiments, 2250 ± 180 mmolSi m^{-2}, than in rice ones, 1460 ± 270 mmolSi m^{-2}. The $\delta^{30}Si$ in rice compartments evolves from about 1 ‰ in the straw to 2 ‰ in the whole grain (Table), in agreement with the enrichment of heavy isotopes observed in the highest parts of the plant (Ding et al., 2005; 2008, Sun et al., 2008; 2016). Bulk rice $\delta^{30}Si$ of rice experiments, 1.29 ± 0.07 ‰, is significantly different from the bulk rice of rice+DE experiments, 0.99 ± 0.07 ‰. Both are 1 ‰ higher than the values observed up to now in rice, all close to 0 ‰ (Ding et al., 2005; 2008, Sun et al., 2008).

The $ASi_{ZB\ corr}$ fractions of the four algal mats (one per experiment) range between 0.7 (rice+DE) to 2.0 % (bare+DE) (Table 4). Although the presence of few diatom frustules in

algal mats was attested by scanning electron microscopy, the $ASi_{ZB\ corr}$ contents in algal mats is not significantly different from soils. One reason could be that because soil ASi is high, the algae bloom has little effect on the total ASi at soil surface. Three over the four $\delta^{30}Si$ of algal mat ASi_{ZB} fall within a mixing between clays and a range of ASi end-member from +0.5 to +1.5 ‰ (Fig. 4), encompassing the straw $\delta^{30}Si$ (+1 ‰). In absence of pure algae analysis, some uncertainty remains on the $\delta^{30}Si$ of algal mat ASi_{ZBcorr}.

3 Discussion

3.1 Validation of Na- and Cl-based mass balances

The high DSi and Na concentrations in the bore-well makes irrigation the unique solute source (>99 %) of these elements to the plot (Table 2). Bore-well represents also the dominant source of Cl (93 %) and makes the KCl contribution marginal (~6 %) although this latter is still 12 times higher than the rainwater contribution (0.5 %). Such situation is representative of the intensive agriculture context in Peninsular India, which relies massively on bore-well irrigation since two decades (Shah, 2014) and is responsible for the degradation of groundwater quality (Siva Soumya et al., 2013; Buvaneshwari et al., 2017). Applying CMB method in this context is unusual, as in most systems studied up to now it was considered that Cl originates only from the atmosphere (Dettinger 1989, Maréchal et al., 2009) or from KCl (Tyner et al., 2000). Since bore well water composition was stable over the duration of the experiment, the Si, Cl and Na input fluxes to each plot could be precisely determined. In the stagnant water (above-ground samples and 1cm-deep Rhizons of all experiments), the covariation of Cl and Na concentrations reflects the evaporation/dilution cycles of the irrigation water (Fig. 2a) and cannot be explained by interactions with soil particles nor plants. Then, above the ground the conservative behavior of Cl and Na is validated, confirming their pertinence for estimating the evaporation at the ground surface (Eq. 3) and the DSi removal from stagnant water.

Soil pore waters could be recovered only once during the reproducing stage, i.e. when the rice plants had grown up, which is a possible limitation of the approach. Taken as a whole, chemical composition of pore waters displays a Na vs Cl relationship more scattered than for surface waters. Moreover, the deepest pore waters from the rice experiments plot above the area defined by above-ground waters (Fig. 2c). This relative Na-enrichment can be explained by Na addition and/or a Cl removal from pore water combined with high evapotranspiration.

Since the main source of Na in local soils is Na-plagioclase (Riotte et al., 2014), Na addition would imply a slight but significant weathering of this primary mineral in rice experiments. Alternatively, a combination of partial Cl removal by plant uptake with high evapotranspiration would be consistent with (1) the evapotranspiration intensity at the period of coring which is known to be maximum at this crop stage III (reproductive; e.g. Tyagi et al., 2000) and (2) the soil-to-plant transfer of chloride of 5% and the Cl concentrations in above-ground rice biomass, from 0.14 g kg^{-1} dry wt in polished rice to 4.8 g kg^{-1} in roots (Tsukada and Takeda, 2008). While it was not possible to quantify the extent of Na addition and/or Cl removal, the soil pore water compositions at least indicate that in rice experiments Na and/or Cl are not conservative. The main consequence for the solute mass balance within the soil layer of this experiment should be an underestimation (Na-based) or an overestimation (Cl-based) of soil leaching water flux. Indeed, Cl-based and Na-based soil leaching fluxes, 457 and 229 mm respectively, flank the value deduced from actual evapotranspiration, 391 mm. Although the relative uncertainty on the soil leaching water flux is large, the incidence on the Si solute budget is limited because of the low DSi concentrations of deep soil pore waters. According to the calculation of water flux, soil leaching Si flux in the rice experiment range only from 30 to 55 mmolSi m^{-2}. Then, the DSi flux removed from the soil layer, calculated by difference between DSi soil input and output would only range within 210 and 240 mmolSi m^{-2}, under the conditions which this mass balance was performed, i.e. in absence of monitoring of soil pore water composition. To summarize, Na and Cl exhibit conservative behaviors above the ground but not within the soil layer of rice experiments. Nevertheless, because Na and Cl behave in opposite ways, the former slightly added to the system and the latter slightly removed, they can provide a range for the soil leaching water flux. The precision associated to a solute budget within the soil layer, deduced from Na and Cl mass balance, shall mostly depend on the difference between input and output DSi concentrations.

3.2 Controls of DSi and δ^{30}Si- DSi above the ground surface

Solute budgets indicate that above-ground processes affect DSi mass balance of all experiments, with different intensities for bare and rice experiments but no visible influence of DE addition. Two processes could be envisaged for explaining above-ground DSi removal in bare plots, diatom uptake and/or adsorption on Fe-oxyhydroxides. Since soil Si pools are large compared to the DSi flux removed during a cropping season, none of these processes is expected to significantly change the size or the isotopic composition of soil pools. For

518 instance, if DSi removal would only originate from diatom blooms, the algal mat would
519 contain at best 10% more ASi than the soil if the sample collected at the ground surface would
520 be 3mm thick. Such a limited increase lies within the incertitude of ASi determination and
521 prevents quantification of this process, although few diatom frustules were observed by
522 scanning electron microscope. An alternative way to assess the importance of diatom uptake
523 and/or adsorption on Fe-oxyhydroxides is to consider the kinetics of these processes. In batch
524 experiments with solid/liquid ratio as low as 1/250 and similar initial DSi concentration,
525 Delstanche et al. (2009) observed that 40% of DSi is absorbed onto Ferrihydrite after 72 hours
526 and 25% onto Goethite after 500 hours. In paddy field conditions where the solid/liquid ratio
527 is ten to hundred times higher than in this batch experiment, DSi removal rate should increase
528 in same proportions as the solid/liquid ratio and induce a drop in DSi within few hours after
529 irrigation.
530 During these experiments, the level of DSi in 1cm-Rhizons or above-surface samples was
531 nearly always depleted compared to the borewell, even when waters were collected soon after
532 irrigation. The intensity and rate of DSi removal is visible when DSi is compared to Na
533 concentrations (Fig. 2b): for most samples, DSi drops while Na remains at the borewell
534 concentration. For instance, a 30% DSi depletion was observed within the 100 m-long open
535 channel separating the bore-well from the experimental plots, during a previous experiment
536 (the channel was replaced by a pipe avoid Si depletion by delivering irrigation water directly
537 to the plot, Fig. 2b) which attests that DSi depletion is almost immediate and incompatible
538 with the timescale of diatom growth, typically few days whatever the temperature, nutrient
539 and light conditions (e.g. Litchman et al., 2003; Schabhüttl et al., 2013).
540 The DSi removal above the ground surface fractionates Si isotopes according to an isotopic
541 fractionation factor ($^{30}\varepsilon$) that depends upon the process at stake. For instance, $^{30}\varepsilon$ induced by
542 diatom uptake (-1.12 ± 0.2 ‰, Alleman et al., 2005; -1.04 ± 0.08 ‰, Opfergelt et al., 2011)
543 and adsorption onto ferrihydrite (-1.08 ± 0.06 ‰, Delstanche et al., 2009) induce smaller
544 isotopic fractionation than Si adsorption onto goethite (-1.62 ± 0.24 ‰; Delstanche et al.,
545 2009). Thanks to the solute mass balance (see section 3.2), the residual fraction of DSi in
546 above-ground water could be estimated for each sample and the $^{30}\varepsilon$ of above-ground DSi
547 removal deduced graphically using the initial borewell composition, the DSi-δ^{30}Si and the
548 residual fractions of DSi. Residual fractions of DSi were calculated by three ways, (1)
549 considering Na as conservative element (Fig. 5a), (2) considering Cl as conservative element
550 (Fig. 5b) and (3) directly from the DSi fraction (Fig. 5c). It can be seen from Fig. 5 that

551 $^{30}\varepsilon$ vary slightly according to the way residual fraction is calculated. However, several
552 consistent insights can be drawn from these graphs. First, data fit better a Rayleigh model than
553 a steady state one, particularly bare experiments which display higher DSi-δ^{30}Si than rice
554 ones and larger isotopic fractionation factors, between -1.5 to -2.5 ‰ depending on residual
555 fraction calculation (considering the 1cm rhizon of bare experiment (B) as an outlier in Fig.
556 5a and 5b). These values confirm that the evolution of DSi and DSi-δ^{30}Si above the ground
557 surface cannot be explained by diatom uptake. Indeed, the fast decrease of DSi above the
558 ground even led in several samples to isotopic fractionations even larger than those expected
559 from adsorption onto goethite. This could be linked to the kinetics itself that would enhance
560 preferential removal of light isotopes compared to ^{30}Si. Second, in rice experiments the
561 apparent isotopic fractionation factors were smaller than in bare ones and ranged between -1
562 (value for rice; Ding et al.; 2008) and -1.5 ‰, which means that in rice and rice+DE
563 experiments both plant uptake and adsorption compete for DSi removal. Since the $^{30}\varepsilon$ of DSi
564 removal in rice experiments is close to -1 ‰ (value for rice plant), it is likely that plant uptake
565 dominates DSi removal. Therefore, it will be assumed in the further discussion that above-
566 ground plant uptake ranges from 140 to 270 mmolSi m^{-2}. Third, in agreement with the above
567 ground-surface DSi solute mass balance (Table 3), the DE application did not impact the DSi
568 above-ground budget nor DSi-δ^{30}Si which confirms that above-ground processes do not
569 involve soil particles dissolution.
570
571
572 In regions covered with paddy fields, irrigation water is transported by canal from the river to
573 the paddy fields located at the highest topographical position and then passes by gravity
574 through many terraces before returning to the river. It is then likely that interactions of
575 irrigation water with the succession of soil surfaces should amplify the Si adsorption onto Fe-
576 oxy-hydroxides. According to the batch experiments of Delstanche et al. (2009), the fraction
577 of DSi removed by adsorption onto Fe-hydroxides depends on the initial DSi concentration.
578 In the case of goethite, the fraction adsorbed is inversely proportional to the initial DSi, and
579 can reach >70% when initial DSi is 210 µmol L^{-1} (lowest initial DSi tested by these authors),
580 against 45% for an initial DSi of 1290 µmol L^{-1}. Although the trend is less clear for
581 ferrihydrite experiments, DSi adsorption still accounts for more than 60% for the lowest
582 initial DSi concentration. According to the compilation from Gaillardet et al. (1999), DSi of
583 major rivers rarely exceeds 200 µmol L^{-1}, the world average being only 127 µmol L^{-1}. Low
584 DSi in rivers could then contribute to increase the proportion of adsorbed DSi in regions

where paddy fields are irrigated by surface water. In this context, our field experiments and the adsorption experiments of Delstanche et al. (2009) provide an alternative or at least additional explanation for the heavy $\delta^{30}Si$ observed in Asian rivers like the Yangtze River (Ding et al., 2004), the Nile River (Cockerton et al., 2013) or some tributaries of the Ganga (Fontorbe et al., 2013, Frings et al., 2015) where paddy fields and wetlands are widespread. The extreme $\delta^{30}Si$ values downstream the Yangtze River for instance, up to 3.7‰, fall within the range observed in the 1cm rhizons and above-surface waters of our experiments. If they were assigned to plant uptake in paddy fields and wetlands by Ding et al. (2004), we suggest here that these $\delta^{30}Si$ values result at least partly from Si absorption onto soil particles. In these regions, both processes contribute to large DSi removal from aquatic systems, unlike what is observed in temperate climate for instance (Clymans et al., 2011). More detailed studies would be needed to estimate the respective roles of adsorption and plant uptake on extreme riverine $\delta^{30}Si$ values in basins where paddies and/or wetlands are widespread.

3.3 Controls of DSi and δ^{30}Si- DSi within the soil

Depending of leaching calculation methods, the DSi flux leached from the 20cm topsoil layer ranges from 30-55 mmolSi m^{-2} (rice) to 40-80 mmolSi m^{-2} (bare+DE) (Table 3), which overall corresponds to 5 to 15% of the initial DSi supply to each plot. DSi leaching from bare+DE and rice+DE experiments are slightly higher than from bare and rice experiments, indicating that the DE applied may have contributed to DSi budget and plant uptake in the 20 cm topsoil layer. Such values are nearly three orders of magnitude lower than those proposed by Nguyen et al. (2016) from HYDRUS modeling in a Vietnamese crop experiment but closer to the solute balance performed by Klotzbücher et al. (2015) in Philippines, i.e. more humid climate than Mandya. The apparent DSi flux removed from the soil layer (ΔFSi, corresponding to the difference, in Table 3, between soil input and soil output) is paradoxically higher in bare and bare+DE experiments (275-325 and 255-300 mmolSi m^{-2}, respectively) than in rice and rice+DE experiments (210-240 and 190-245 mmolSi m^{-2}, respectively). However, if one includes the additional 140 to 270 mmolSi m^{-2} taken up by rice plant above soil surface (see previous section), the ΔFSi values are equivalent for all experiments. As for the above-ground balance, this does not mean that the processes responsible for the DSi removal in bare and rice experiments are the same.

In bare experiments, the smooth decrease of DSi with depth corresponds to a process occurring along with water percolation, such as DSi adsorption and clay minerals

precipitation. However, according to the Si isotopic fractionation factors estimated up to now for DSi adsorption ($^{30}\varepsilon = -1$ ‰; Delstanche et al., 2009; Opfergelt et al., 2009) or clay minerals formation ($^{30}\varepsilon$ = -1 to -2 ‰; Ziegler et al., 2005; Georg et al., 2007; Méheut et al., 2007), these two processes should have depleted the residual soil pore water in light Si isotopes and then induce an increase of δ^{30}Si-DSi. Instead, δ^{30}Si decreased by about 1 ‰ between soil surface and 15-20 cm depth. The theoretical δ^{30}Si associated to the DSi removal ($\delta^{30}Si_{\Delta FSi}$, calculated with Eq. 6) in bare and bare+DE experiments would then range from 3.70 to 3.84 ‰ and from 4.53 to 4.80 ‰ (Table 3), respectively; i.e. 0.1 to 0.4 ‰ higher than the δ^{30}Si of the input flux. Such signatures are incompatible with the signatures measured in the soil silica pools, which suggests that Si removal is not the unique process controlling DSi and δ^{30}Si-DSi in the soil. The δ^{30}Si-DSi values points to concomitant, isotopically light silica release from soil particles like Si desorption (then partial isotopic exchange during DSi adsorption) or mineral dissolution. Desorption would mean silica exchange with the adsorbed pool of Si of the soil. Since the isotopic signature of the exchangeable pool cannot be determined, the extent of this process cannot be assessed. However, its effect on δ^{30}Si-DSi was already suspected during an adsorption experiment performed on lateritic soils of Cameroon (Opfergelt et al., 2009). The soil silicates susceptible to weather and release silica encompass primary minerals (quartz, Na-plagioclase), secondary clay minerals and opal (ASi). According to the saturation indexes calculated by PHREEQS, quartz and clay minerals would be stable but soil pore waters would be undersaturated regarding to ASi (-0.5 to -0.7) and Na-plagioclase (-13 to -15 assuming Al concentration of 1 ppm). Na-plagioclase weathering could be consistent with the Na excess observed in soil pore waters (Fig. 2c), but both ASi dissolution and Na-plagioclase weathering are expected to contribute to soil DSi.

In rice experiments, the DSi drop just below ground-surface to values as low as 100 µmol L^{-1} or less, was also observed in hydroponic conditions (Ding et al., 2008). Both Na and Cl concentrations increase while DSi decreases which confirms that Si uptake by the rice plant is predominantly selective and then occurs via an active mechanism (e.g. Sun et al., 2016). Because of the Si uptake efficiency, the plants could bring pore water DSi concentration low enough to modify the saturation regarding soils minerals. In several samples DSi was for instance lower than saturation with quartz (100 µmol L^{-1}). The few pore waters recovered by hydraulic press (labelled "HP" in Table 2) systematically exhibited lower concentration than centrifuged ones; the water located in the smallest pores, where roots are more susceptible to

take up nutrients, are indeed more Si depleted than in macro-pores. It is then possible that the undersaturation with soil minerals is more pronounced in these pores than in macro porosity.

3.4 Isotopic mass balance of rice and possible Si sources

Estimating the Si sources to rice plant is possible because the cumulated uncertainty associated to adsorption and soil leaching flux has a little impact on the estimation of DSi contribution to plant uptake, which ranges from 25 to 35 % in rice experiments and from 15 to 23 % in rice+DE ones. The soil pool contributing to plant uptake can be assessed once deduced in this latter the contribution of irrigation DSi. If the total silica taken up by the rice plant (FSi_{plant}) is considered as mix of silica coming from irrigation water (ΔFSi) and from soil mineral weathering, its isotopic composition can be described as:

$$\delta^{30}Si_{plant} = \frac{\Delta DSi.\delta^{30}Si_{F\Delta DSi} + (FSi_{plant} - F\Delta DSi).\delta^{30}Si_{soil\,pool}}{FSi_{plant}} \quad (7)$$

where $\delta^{30}Si_{F_{\Delta}DSi}$ is the δ^{30}Si of irrigation DSi taken up by plants. This isotopic signature can be roughly estimated if one assumes that its evolution during uptake follows a Rayleigh model, which is a working hypothesis, by the relationship:

$$\delta^{30}Si_{F\Delta\mathrm{DSi}} = \delta^{30}Si_{borewell} - {}^{30}\varepsilon_{rice} \cdot f_{F\Delta DSi} \cdot \frac{ln(f_{F\Delta DSi})}{1 - f_{F\Delta DSi}} \quad (8)$$

Where $f_{F\Delta DSi}$ is the fraction of DSi remaining in soil pore water after plant uptake:

$$f_{F\Delta DSi} = \frac{FDSi_{borewell} - FDSi_{plant\,uptake}}{FDSi_{borewell}} \quad (9)$$

According to the ranges of DSi uptake estimated for each experiment, $f_{F\Delta DSi}$ of rice experiment would span from 0.06 to 0.34 and $f_{F\Delta DSi}$ of rice+DE from 0.05 to 0.39. The $\delta^{30}Si_{F_{\Delta}DSi}$ associated to DSi uptakes (Eq. 8), using the ${}^{30}\varepsilon_{rice}$ range from -0.4 to -1 ‰ (Sun et al., 2016), would be equivalent for rice and rice+DE experiments, from 0.93 to 1.42 ‰ and

677 from 0.89 to 1.43 ‰, respectively. Then, the isotopic signature of the complementary soil
678 source to the plant ($\delta^{30}Si_{soil\ pool}$) can be estimated according to the equation:

679

680 $$\delta^{30}Si_{soil\ pool} = \frac{FSi_{plant}.\delta^{30}Si_{plant} - \Delta FSi.\delta^{30}Si_{\Delta FSi}}{FSi_{plant}-\Delta FSi} \qquad (10)$$

681

682 The $\delta^{30}Si_{soil\ pool}$ of rice and rice+DE experiments would then range from 1.22 to 1.41 ‰
683 and from 0.75 to 1.01 ‰, respectively. Accordingly, the complete isotopic mass balance of Si
684 at the soil-plant scale can be summarized (Fig. 6).
685 These heavy isotopic signatures confirm that clay and primary minerals do not significantly
686 contribute to plant-Si. Without discarding a slight contribution of particle desorption, of
687 which the δ^{30}Si cannot be measured or assessed, the closest δ^{30}Si among soil Si pools and
688 most likely soil source would then be soil ASi. This finding is indeed consistent with the
689 saturation index of soil pore water regarding to opal (see previous section) and with the
690 dissolution rate of ASi; According to batch experiments performed by Fraysse et al, (2009),
691 phytolith dissolution rates at circum neutral pH are several order of magnitude higher than
692 those of kaolinite or plagioclase. It is then likely that the relative excess of Na compared to Cl
693 in soil pore water would rather correspond to a slight Cl depletion. The isotopic fingerprint of
694 ASi in rice plant confirms the role of this specific soil pool as source of Si in rice, as proposed
695 by some authors from solute mass balance (e.g. Desplanques et al., 2006). However, it should
696 be stressed that contrary to Camargue or other places where irrigation DSi is low and rice
697 straw removed from field, leading to ASi depletion in these soils, the soil ASi contents in soils
698 of our study were remarkably high because of local practices. In our context, the risk of ASi
699 depletion in soils is limited, although rice cultivation is intensive. The δ^{30}Si of rice plants is
700 sensitive to the most available Si of the soil, as illustrated by the $\delta^{30}Si_{soil\ pool}$ of both
701 experiments that do no overlap with values in rice+DE experiment about -0.3 ‰ lower than
702 those of rice one. The amount of Si applied by DE corresponds to only 14% of biomass-Si in
703 rice+DE and does not explain the 54% difference with rice experiment. But the δ^{30}Si of DE, -
704 0.36 ‰, was contrasted enough to slightly influence the isotopic signature of biomass in
705 rice+DE. Then, it is likely that DE was at least partly incorporated by the plant as a
706 supplementary source of Si and played a role of priming effect, as for N fertilizer (e.g.
707 Jenkinson et al., 1985; Kuzyakov et al., 2000), which induced a higher Si uptake by the plant.

708 The main implication of this isotopic mass balance is that rice could be able to take Si from a
709 solid source (ASi) without significant isotopic fractionation. Finally, replicating such
710 experiments in conditions of low silica availability (ASi-poor soils and irrigation with low
711 DSi water) would probably reveal a different distribution of silica sources to the plant.
712

713 # 4 Conclusion

714 By combining data on water, soil and plants we have shown that Si isotopic signatures are
715 useful for constraining the dynamics of Si in a paddy fields. A significant DSi removal
716 occurred very soon after plot irrigation consistent with adsorption in bare soils. Within the soil
717 layer, pore water DSi and $\delta^{30}Si$ exhibited a sharp decrease in rice experiments which
718 illustrated the active DSi uptake by rice within the soil. The DE application was also traced by
719 a slightly lighter Si isotope signature in the soil solution. At the field scale, our results puts
720 constraints for a better understanding on the effects of soil Si application. At the global scale,
721 the results highlight a possible DSi sink in wetlands, even in not vegetated areas, that could be
722 responsible of the high $\delta^{30}Si$ observed in some tropical rivers.
723

724 ***Acknowledgements***
725 The study was supported by the Indo-French Centre for the Promotion of Advanced Research
726 (IFCPAR/CEFIPRA; Project n°5109-1) and the French Institute for Research and
727 Development (IRD, France) which funded deputation of J. Riotte and long duration stays of
728 J.D. Meunier. The authors thank the two anonymous reviews for their useful comments on the
729 manuscript. Hemanth Moger and Jean-Louis Duprey are thanked for the chemical analyses,
730 Jonathan Prunier and Manuel Henry for their support in clean room and the personnel of VC
731 farm at Mandya for their help during the rice cropping experiment.

732 ***References***
733 Alexandre A, Meunier J D, Colin F and Koud J M 1997 Plant impact on the biogeochemical
734 cycle of silicon and related weathering processes. Geochim. Cosmochim. Acta, 6, 677–682
735 Alleman L Y, Cardinal D, Cocquyt C, Plisnier P D, Descy JP, Kimirei I, Sinyinza D and
736 André L 2005 Silicon isotopic fractionation in Lake Tanganyika and its main tributaries. J.
737 Great Lakes Res. 31, 509–519
738 Allen P A 1997 Earth surface processes (p. 404). Oxford: Blackwell.

739 Allen R G, Pereira L S, Raes D and Smith M 1998 Crop evapotranspiration: guidelines for
740 computing crop water requirements. FAO Irrigation and Drainage Paper 56. (FAO, Rome,
741 1998), 326 p

742 Anupama K, Prasad S and Reddy C S (2014) Vegetation, land cover and land use changes of
743 the last 200 years in the Eastern Ghats (southern India) inferred from pollen analysis of
744 sediments from a rain-fed tank and remote sensing, Quat. Int., 325, 93-104

745 Bartoli F, and Wilding L P 1980 Dissolution of Biogenic Opal as a Function of its Physical
746 and Chemical Properties. Soil Sci. Soc. Am. J. 44, 873-878.
747 doi:10.2136/sssaj1980.03615995004400040043x

748 Brenchley W E and Maskell E J 1927 The inter-relation between silicon and other elements in
749 plant nutrition. Ann. Appl. Biol. 14, 45-82

750 Buvaneshwari S, Riotte J, Sekhar M, Mohan Kumar M S, Sharma A K, Duprey J L, Audry S,
751 Giriraja P R, Yerabham P, Moger H, Durand P, Braun J J and Ruiz L 2017 Groundwater
752 resource vulnerability and spatial variability of nitrate contamination: insights from high
753 density tubewell monitoring in a hard rock aquifer. Sci. Tot. Env., 579, 838-847

754 Braun J J, Descloitres M, Riotte J, Fleury S, Barbiero L, Boeglin J L, Violette A, Lacarce E,
755 Ruiz L, Sekhar M, Mohan Kumar M S, Subramanian S and Dupré B 2009 Regolith mass
756 balance inferred from combined mineralogical, geochemical and geophysical studies: Mule
757 Hole gneissic watershed, South India. Geochim. Cosmochim. Acta 73, 935-961

758 Cardinal D, Gaillardet J, Hughes H J, Opfergelt S and André L 2010 Contrasting silicon
759 isotope signatures in rivers from the Congo Basin and the specific behaviour of organic-rich
760 waters. Geophys. Res. Lett. 37, doi:10.1029/2010GL043413

761 Cary L, Alexandre A, Meunier J D, Boeglin J L and Braun J J 2005 Contribution of phytoliths
762 to the suspended load of biogenic silica in the Nyong basin rivers (Cameroon).
763 Biogeochem.74, 101–114

764 Cheng B T 1982 Some significant functions of silicon to higher plants. J. Plant Nutr. 5, 1345-
765 1353

766 Clymans W, Struyf E, Govers G, Vandevenne F and Conley D J 2011 Anthropogenic impact
767 on biogenic Si pools in temperate soils. Biogeosciences 8, 2281–2293

768 Cockerton H E, Street-Perrott F A, Leng M J, Barker PA, Horstwood M S A and Pashley V
769 2013 Stable-isotope (H, O, and Si) evidence for seasonal variations in hydrology and Si

770 cycling from modern waters in the Nile Basin: implications for interpreting the Quaternary
771 record. Quat. Sci. Rev. 66, 4–21
772 Crooks R and Prentice P 2016 Extensive Investigation Into Field Based Responses to a Silica
773 Fertiliser. Silicon 9, 301-304, DOI: 10.1007/s12633-015-9379-3
774 Datnoff L E and Rodrigues F A 2005 The role of silicon in suppressing rice diseases. APS net
775 Feature Story, 1-28, http://www.apsnet.org/online/feature/silicon/
776 Delstanche S, Opfergelt S, Cardinal D, Elsass F, André L and Delvaux L 2009 Silicon
777 isotopic fractionation during adsorption of aqueous monosilicic acid onto iron oxide.
778 Geochim. Cosmochim. Acta, 73, 923-934
779 Demarest M S, Brzezinski M A and Beucher C P 2009 Fractionation of silicon isotopes
780 during biogenic silica dissolution. Geochim. Cosmochim. Acta, 73, 5572–5583
781 Derry L A, Kurtz A C, Ziegler K and Chadwick O A (2005) Biological control of terrestrial
782 silica cycling and export fluxes to watersheds. Nature, 433, 728-731
783 Desplanques V, Cary L, Mouret J C, Trolard F, Bourrie G, Grauby O and Meunier J D 2006
784 Silicon transfers in a rice field in Camargue (France). J. Geochem. Explor. 88, 190-193
785 Dettinger M D 1989 Reconnaissance estimates of natural recharge to desert basins in Nevada,
786 USA, by using chloride-balance calculations. J. Hydrol. 106, 55–78
787 Dietrich D, Hinke S, Baumann W, Fehlhaber R, Bäucker E, Rühle G, Wienhaus O. and Marx
788 G 2003 Silica accumulation in Triticum aestivum L. and Dactylis glomerata L. Anal. Bioanal.
789 Chem. 376, 399-404
790 Ding T, Wan D, Wang C and Zhang F 2004 Silicon isotope compositions of dissolved and
791 suspended matter in the Yangtze River, China. Geochim. Cosmochim. Acta 68, 205-216
792 Ding T, Ma G, Shui M, Wan D and Li R 2005 Silicon isotope study on rice plants from the
793 Zhejiang province, China. Chem. Geol. 218, 41-50
794 Ding T, Tian S H, Sun L, Wu L H, Zhou J X and Chen ZY 2008 Silicon isotope fractionation
795 between rice plants and nutrient solution and its significance to the study of the silicon cycle.
796 Geochim. Cosmochim. Acta 72, 600–615
797 Fontorbe G, De La Rocha C, Chapman H J and Bickle M J 2013 The silicon isotopic
798 composition of the Ganges and its tributaries. Earth Planet. Sci. Lett. 381, 21–30
799 Fouépé Takounjou A, Ndam Ngoupayou J R, Riotte J, Takem G E, Mafany G, Maréchal J C
800 and Ekodeck G E 2011 Estimation of groundwater recharge of shallow aquifer on humid

environment in Yaoundé, Cameroon using hybrid water fluctuation and hydrochemistry methods. Environ. Earth. Sci., 64, 107-118

Fraysse F, Pokrovsky O S, Schott J and Meunier J D 2009 Surface chemistry and reactivity of plant phytoliths in aqueous solutions. Chem. Geol. 258, 197–206

Frings P J, Clymans W and Conley D J 2014 Amorphous silica transport in the Ganges basin: Implications for Si delivery to the oceans. Proc. Earth Planet. Sci. 10, 271-274

Frings P J, Clymans W, Fontorbe G, Gray W, Chakrapani G J, Conley D J and De La Rocha C L 2015 Silicate weathering in the Ganges alluvial plain. Earth Planet. Sci. Lett. 427, 136–148

Frings P J, Clymans W, Fontorbe G, De La Rocha C L and Conley C L 2016 The continental Si cycle and its impact on the ocean Si isotope budget. Chem. Geol. 425, 12–36

Gaillardet J, Dupré B, Louvat P and Allègre C J 1999 Global silicate weathering and CO_2 consumption rates deduced from the chemistry of large rivers, Chem. Geol. 159, 3-30

Georg R B, Reynolds B C, Frank M and Halliday A N 2006 Mechanisms controlling the silicon isotopic compositions of river waters. Earth Planet. Sci. Lett. 249, 290-306

Georg R B, Reynolds B C, West A J, Burton K W and Halliday A N 2007 Silicon isotope variations accompanying basalt weathering in Iceland. Earth Planet. Sci. Lett. 261, 476–490

Guntzer F, Keller C and Meunier J D 2012 Benefits of plant silicon for crops: a review. Agronomy Sust. Dev. 32, 201-213

Henriet C, Bodarwé L, Dorel M, Draye X and Delvaux B 2008 Leaf silicon content in banana (Musa spp.) reveals the weathering stage of volcanic ash soils in Guadeloupe. Plant and Soil, 313, 71-82, DOI 10.1007/s11104-008-9680-7

Hughes H J, Sondag F, Cocquyt C, Laraque A, Pandi A, André L and Cardinal D 2011 Effect of seasonal biogenic silica variations on dissolved silicon fluxes and isotopic signatures in the Congo River. Limnol. Oceanogr., 56, 551–561

Hughes H J, Sondag F, Santos R V, André L and Cardinal D 2013 The riverine silicon isotope composition of the Amazon Basin. Geochim. Cosmochim. Acta 121, 637-651

Irfan K, Trolard F, Shahzad T, Cary L, Mouret JC and Bourrié G 2017 Impact of 60 Years of Intensive Rice Cropping on Clay Minerals in Soils Due to Si Exportation. American Journal of Agriculture and Forestry 5, 40-48

Jenkinson D S, Fox R H and Rayner J H 1985 Interactions between fertilizer nitrogen and soil nitrogen- the so-called ‘priming’ effect. Eur. J. of Soil Sci. 36, 425–444

833 Klotzbücher T, Leuther F, Marxen A, Vetterlein D, Horgan F G and Jahn R 2015 Forms and
834 fluxes of potential plant-available silicon in irrigated lowland rice production (Laguna, the
835 Philippines). Plant and Soil DOI 10.1007/s11104-015-2480-y
836 Kuzyakov Y, Friedel J K and Stahr K 2000 Review of mechanisms and quantification of
837 priming effects. Soil Biology & Biochemistry, 32, 1485-1498
838 Liang Y, Nikolic M, Belanger R, Haijun G and Song A 2015 Silicon in Agriculture. From
839 Theory to Practice. Dordrecht: Springer
840 Litchman E, Steiner D and Bossard P 2003 Photosynthetic and growth responses of three
841 freshwater algae to phosphorus limitation and daylength. Freshwater Biology, 48, 2141–2148
842 Lucas Y 2001 The role of plants in controlling rates and products of weathering: Importance
843 of Biological pumping. Annu. Rev. Earth Planet. Sci. 29, 135-163
844 Ma J F and Takahashi E 2002 Soil, fertilizer, and plant silicon research in Japan. Elsevier,
845 Amsterdam. 281p
846 Makabe S, Kakuda K, Sasaki Y, Ando T, Fujii H and Ando H 2009 Relationship between
847 mineral composition or soil texture and available silicon in alluvial paddy soils on the
848 Shounai Plain, Japan. Soil Sci. Plant Nutr. 55, 300-308
849 Maréchal J C, Murari R R V, Riotte J, Vouillamoz J M, Mohan Kumar M S, Ruiz L, Muddu S
850 and Braun J J 2009 Indirect and direct recharges in a tropical forested watershed: Mule Hole,
851 India. J. Hydrol. 364, 272-284
852 Maréchal J C, Braun J J, Riotte J, Bedimo Bedimo J P and Boeglin J L 2011a Hydrological
853 Processes of a Rainforest Headwater Swamp from Natural Chemical Tracing in Nsimi
854 Watershed, Cameroon. Hydrol. Process. 25, 2246-2260
855 Maréchal J C, Riotte J, Lagane C, Subramanian S, Kumar C, Ruiz L, Audry S, Murari V and
856 Braun JJ 2011b Chemical groundwater outputs from a small drainage watershed: Mule Hole,
857 South India. Appl. Geochem. 26, S94-S96
858 Méheut M, Lazzeri M, Balan E and Mauri F 2007 Equilibrium isotopic fractionation in the
859 kaolinite, quartz, water system: prediction from first-principles density-functional theory.
860 Geochim. Cosmochim. Acta 71, 3170–3181
861 Meunier J D, Guntzer F, Kirman S and Keller C 2008 Terrestrial plant-Si and environmental
862 changes. Miner. Mag. 72, 263-267

Meunier J D, Riotte J, Braun J J, Muddu S, Chalié F, Barboni D and Saccone L 2015 Controls of DSi in streams and reservoirs along the Kaveri River, South India. Sci. Tot. Env. 502, 103-113

Meunier J D, Barboni D, Anwar-ul-Haq M, Levard C, Chaurand P, Vidal V, Grauby O, Huc R, Laffont-Schwob I, Rabier J and Keller C 2017 Effect of phytoliths for mitigating water stress in durum wheat. New Phytol, 215: 229–239. doi:10.1111/nph.14554

Nguyen N M, Dultz S, Picardal F, Bui A T K, Pham Q V, Dam T T N, Nguyen C X, Nguyen N T and Bui H T 2016 Simulation of silicon leaching from flooded rice paddy soils in the Red River Delta, Vietnam. Chemosphere, 145, 450-456

Opfergelt S, de Bournonville G, Cardinal D, André L, Delstanche S and Delvaux B 2009 Impact of soil weathering degree on silicon isotopic fractionation during adsorption onto iron oxides in basaltic ash soils, Cameroon. Geochim. Cosmochim. Acta. 73, 7226–7240

Opfergelt S, Eiriksdottir E S, Burton K W, Einarsson A, Siebert C, Gislason S R and Halliday A N 2011 Quantifying the impact of freshwater diatom productivity on silicon isotopes and silicon fluxes: Lake Myvatn, Iceland. Earth Planet. Sci. Lett. 305, 73–82

Opfergelt S. and Delmelle P. (012 Silicon isotopes and continental weathering processes: Assessing controls on Si transfer to the ocean. C. R. Geoscience 344, 723–738

Pati S, Pal B, Badole S, Hazra G C and Mandal B 2016 Effect of Silicon Fertilization on Growth, Yield, and Nutrient Uptake of Rice, Commun. Soil Sci. Plant Anal., 47, 284-290

Piperno D R 1988 Phytolith Analysis: An Archaeological and Geological Perspective. Academic Press, San Diego, 280 p

Reddy K C, Arunajyothy S and Mallikarjuna P 2015 Crop Coefficients of Some Selected Crops of Andhra Pradesh. J. Inst. Eng. India Ser. A, 96, 123–130

Riotte J, Maréchal J C, Audry S, Kumar C, Bedimo J P, Ruiz L, Sekhar M, Cisel M, Chitra Tarak R, Varma M R R, Lagane C, Reddy P and Braun J J (2014) Vegetation impact on stream chemical fluxes: Mule Hole watershed (South India). Geochim. Cosmochim. Acta 145, 116-138

Sandhya K. 2016 Biogeochemistry of silicon in different rice ecosystems of Karnataka. Ph.D. Thesis, Univ. Agric. Sci., Bengaluru, Karnataka, India

Savage P.S., Georg R.B., Williams H.M., Turner S., Halliday A.N. and Chappell B.W.(2012 The silicon isotope composition of granites. Geochim. Cosmochim. Acta, 92, 184-202

894 Savant N K, Datnoff L E and Snyder G H 1997 Depletion of plant available silicon in soils: A
895 possible cause of declining rice yields, Comm. Soil Sci. Plant Anal., 28, 1245-1252
896 Schabhüttl S, Hingsamer P, Weigelhofer G, Hein T, Weigert A and Striebel M 2013
897 Temperature and species richness effects in phytoplankton communities. Oecologia, 171,
898 527–536. DOI 10.1007/s00442-012-2419-4
899 Seyfferth A L, Kocar B D, Lee J A and Fendorf S 2013 Seasonal dynamics of dissolved
900 silicon in a rice cropping system after straw incorporation. Geochim. Cosmochim. Acta 123,
901 120–133
902 Shah T. 2014 Groundwater Governance and Irrigated Agriculture. Stockholm, Sweden:
903 Global Water Partnership, Technical Committee (TEC).. 71p. (TEC Background Papers 19)
904 doi:10.1080/09614520701469427
905 Siva Sivapalan 2015 Water Balance of Flooded Rice in the Tropics, Irrigation and Drainage -
906 Sustainable Strategies and Systems, Muhammad Salik Javaid (Ed.), InTech, DOI:
907 10.5772/59043
908 Siva Soumya B, Sekhar M, Riotte J, Banerjee A and Braun J J 2013 Characterization of
909 groundwater chemistry under the influence of lithologic and anthropogenic factors along a
910 climatic gradient in Upper Cauvery basin, South India. Env. Earth Sci., 69, 2311–2335
911 Struyf E, Smis A, Van Damme S, Garnier J, Govers G, Van Wesemael B, Conley D J,
912 Batelaan O, Frot E, Clymans W, Vandevenne F, Lancelot C, Goos P and Meire P 2010
913 Historical land use change has lowered terrestrial silica mobilization. Nat. Comm. 1, 129
914 Sun L, Wu L H, Ding T P and Tian S H 2008 Silicon isotope fractionation in rice plants, an
915 experimental study on rice growth under hydroponic conditions. Plant and Soil 304, 291–300.
916 DOI 10.1007/sl 11 04-008-9552-1
917 Sun Y, Wu L H and Li X 2016 Experimental Determination of Silicon Isotope Fractionation
918 in Rice. PLoS ONE 11(12): e0168970. doi:10.1371/journal.pone.0168970
919 Tyagi N K, Sharma D K and Luthra S K 2000 Determination of evapotranspiration and crop
920 coefficients of rice and sunflower with lysimeter. Agri. Water Manag. 45, 41-54
921 Tyner J. S., Brown G. O., Vogel J. R., Garbrech J. 2000 Chloride mass balance to determine
922 water fluxes beneath KCl-fertilized crops. Trans. ASABE 43, 1553–1559
923 doi:10.13031/2013.3055

924 Vandevenne F I, Struyf E, Clymans W and Meire P 2012 Agricultural silica harvest: have
925 humans created a new loop in the global silica cycle? Frontiers in Ecology and the
926 Environment, 10, 243–248, doi:10.1890/110046
927 Vandevenne F I, Barão L, Ronchi B, Govers G, Meire P, Kelly E F and Struyf E 2015a
928 Silicon pools in human impacted soils of temperate zones. Global Biogeochem. Cycles, 29,
929 doi:10.1002/2014GB005049
930 Vandevenne F I, Delvaux C, Hughes H J, André L, Ronchi B, Clymans W. Barão L, Cornelis
931 J T, Govers G, Meire P and Struyf E 2015b Landscape cultivation alters δ^{30}Si signature in
932 terrestrial ecosystems. Scientific reports, 5: 7732, DOI: 10.1038/srep07732
933 Zambardi T and Poitrasson F 2011 Precise Determination of Silicon Isotopes in Silicate Rock
934 Reference Materials by MC-ICP-MS. Geostandards and Geoanalytical Res., 35, 89-99
935 Ziegler K, Chadwick O A, White A F and Brzezinski M A 2005 δ^{30}Si systematics in a granitic
936 saprolite, Puerto Rico. Geology 33, 817–820